Wind-Wise Automated Decision Support Tool for Tower Crane type selection and location

AlaaEldin Hebiba

A Thesis

In the Department

of

Building, Civil and Environmental Engineering

Presented in Partial Fulfillment of the Requirements

For the Degree of

Master of Applied Science in (Construction Engineering) at

Concordia University

Montreal, Quebec, Canada

August 2020

Concordia University

School of Graduate Studies

This is to certify that the thesis prepared

By: AlaaEldin Hebiba

Entitled: Wind-Wise Automated Decision Support Tool for Tower Crane type
                selection and location

and submitted in partial fulfillment of the requirements for the degree of

Master of Applied Science (Construction Engineering)

Signed by the final Examining Committee:

_____Chair

Dr. M. Nik-Bakht

_____Examiner

Dr. Fuzhan Nasiri

_____External Examiner

Dr. Amin Hammad

_____Co-Supervisor

Dr. Ahmed Bouferguene

_____Co-Supervisor

Dr. S. H. Han

Approved by_____

Dr. Michelle Nokken, Graduate Program Director

August 13, 2020 _____

Dr. Amir Asif, Dean, Gina Cody School of Engineering and Computer Science

Abstract

Wind-Wise Automated Decision Support Tool for Tower Crane type selection and location

AlaaEldin Hebiba

Extreme wind speeds pose a serious threat to tower crane stability. Out-of-service wind loads trigger moments that may lead to overturning of a tower crane. Even if the tower crane is anchored to the ground, its structural integrity can be compromised by strong winds since the pressure exerted by the latter can lead to excessive deflections of the mast (which may be a main cause for collapse of the entire structure). Paradoxically, although strong winds have been linked to some catastrophic failures of tower cranes, their effect is often overlooked from a construction management perspective when the models for these cranes are selected during construction planning. Moreover, tower crane location and resources supply locations selection both significantly influence the tower crane model designation and subsequently the overall productivity of the project. This paper proposes a methodology which is consisting of (i) twofold mathematical distance-based-optimization technique encompassing the crane capacity (represented as the lifted moments) and hook operation time to analyze the tower crane site layout combinatorial optimization (determining the optimal crane and the corresponding material supply locations) therefore, facilitating selecting the tower crane model through the lifting critical radius. This optimization gives practitioners the option to explore the effect of different sets of constraints on productivity and overall lifting moments. In this respect, the planning team can choose to favor faster crane operations (i.e., a tighter schedule of crane operations), or they may opt to minimize the lifting-moment, choosing a more conservative crane capacity model to mitigate total cost (ii) a static wind analysis to investigate the efficiency of the tower crane model selected to withstand

extreme wind speeds against overturning (through grounding bearing pressures reactions) and mast excessive deformation (compared to allowable deflection constraints). The proposed methodology is applied on a large-scale construction site with 514 crane and material supply location and the selected tower crane model resistance against maximum potential wind speed is examined and ballast base dimensions are determined. Additionally, a case study from the existing literature is investigated as a small-scale construction site and more improved site layout optimization is generated. Finally, a well-known-real-world crane accident is analyzed to validate the performance of the proposed wind static analysis method.

This Thesis is dedicated to my father "Magdy"; my mother "Nagwa"; my siblings "Amr", "Ali"

and "Ola"; and my niece "Leila".

ACKNOWLEDGEMENTS

Contents

List of Figures

List of Tables

Chapter 1: Introduction

Tower cranes are a key determinant of productivity in high-rise construction projects due to the key role they play in material transportation. Accordingly, effective selection and management of cranes contributes significantly to project success. Presently, tower cranes are increasingly employed in North America for those projects that would traditionally employ mobile cranes, which are potentially more dangerous than tower cranes due to their configuration, operation conditions, and their capability to cope with duty-cycle work [1–4].

Given that the trend is towards large-scale construction, high priority is given to meeting tight deadlines, larger quantities of materials and many workers are involved, construction operations are more intricate, management activities are more complex, and tower cranes are of the utmost significance for any construction project, dominating all other resources within its sphere of influence. Hence, there is a rapidly increasing need for safer, faster, more productive cranes combined with adequate equipment planning and supervision of lifting operations [5,6]. However, continuous tower crane operations are inherently dynamic, complex, poorly judged and supervised; therefore, safety issues are exacerbated. [7] Moreover, exposure to ambient conditions presents yet another set of challenges with respect to crane safety and productivity [8].

At the present time, software and other tools for decision and planning support are becoming more readily available, and modern cranes are furnished with a range of advanced technologies to improve productivity and safety, thanks to advancements in computerization and communication technologies [4]. Researchers have subcategorized crane productivity and safety into a broad set of areas and studies. In terms of safety, the various circumstances and factors that lead to crane failures have motivated numerous studies to evaluate these factors generically and

statistically [1,8–12], while others have investigated individual crane incidents thoroughly. [13–16]

These studies have also encompassed measurements and safety systems. For example, Vision, laser technology, ultra-wide band based and alarm remote monitoring systems have been designed for tracking lifting path [17–20], game-based simulation has been developed for virtual safety training of mantling and dismantling of tower cranes [21] and recommendations have been made for safety legislators and administrations [22,23]. Statistically, 85 tower crane accidents were reported between 1989 and 2009 world-wide [24] Fig 1 shows the factors responsible for tower crane failures that lead to loss of lives and the loss of tens and hundreds of millions of dollars (however, statistical data on accidents may not be a reliable reference due to the large number of unreported incidents). Notwithstanding, depending on statistical data or studies evaluated tower crane accidents causes , wind has been shown to have an enormous impact on crane failure (e.g., Mecca crane catastrophe, Dallas crane collapse) [25,26].
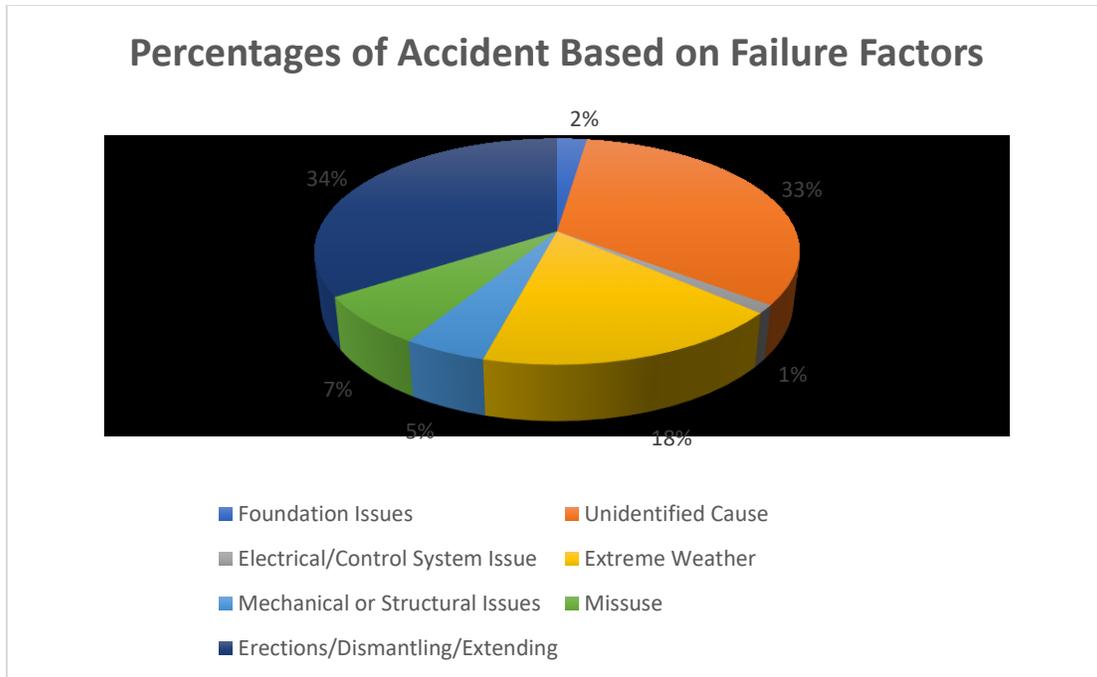
Fig 1 Percentages of different factors involved into tower crane failures

According to statistical data or studies evaluated tower crane accidents causes , wind has been shown to have an enormous impact on crane failure [24]. Meanwhile, approaches to enhance productivity levels and reduce total costs have garnered interest among researchers over the years. Crane operation planning passes through five major processes (crane model, location and supply locations selection – grounding bearing pressure analysis - lifting operations sequence - crane lifting path planning - 3D visualization). Many studies have developed algorithms and approaches regarding the five processes to ultimately enhance productivity levels, reduce total costs and improve safety measures. In terms of crane model, location and supply locations selection, Rodriguez-Ramos and Francis [27] built a mathematical model to reduce operation transportation time. Gray and Little [28] enhanced the model introduced by Furusaka and Gray [29], adding the capability of selecting appropriate number of cranes. Hannah and Lotfallah [30] used fuzzy logic

to select the compatible crane type. Al-Hussein et al. [31] addressed the limitations of lifting capacity charts by introducing a software tool that considers various configuration, crane-site assimilation, and boom and jib clearances supported with AutoCAD simulation. Sawhney and Mund [32] adopted Artificial Neural Networks (ANN) for crane type selection. Huang and Wong [33] have developed Particle Bee algorithm to determine crane and supply locations moreover, minimizing the operating cost.

Regarding grounding pressure analysis, Liu et al. [34] modified traditional bearing capacity equations to address differences of soils for cranes and computer simulation was applied to study the bearing capacity allowed for crawler cranes. Kim et al. [35] suggested an optimization algorithm to select the appropriate design for the fixing anchorage foundation of tower cranes overshadowing the ballast base foundation systems. For Lifting operations sequence, Al-Hussein et al. [36] filled the gap between discrete-event-simulation (DES) and real-world-visualization, integrating Simphony.NET with 3ds Max to generate tower crane lifting scenarios providing more insight into projects productivity. Similarly for mobile cranes, Han et al. [37] combined clearance examination and operation cycle time estimation. Taghaddos et al. [38] presented a simulation-based auction protocol to schedule the supply resources for multiple cranes lifting operations. For crane lift path planning, Reddy and Varghese [39] investigated the implementation of configuration space (C-space) and robotic search concepts to develop an automated path planning tool for crane-based heavy-lift planning with respect to crane capacity with maximum, minimum working radii and clearance limits. Sivakumar et al. [40] compared the capability of a two heuristic search methods Hill climbing and A* for automating path-planning task of cooperative crane lifts. Zhang and Hammad [41] implemented ultra-wideband for supporting crane operators to detect potential collisions. The crane operator can visualize and monitor the crane operations using

Autodesk Softimage. For 3D visualization of crane operations, Wang et al. [42] presented a 3D BIM model integrated with Firefly Algorithm to demonstrate the optimal tower crane layout plan. Kang et al. [43] developed 3D simulation and animation to present an unvague schedule and operations planning for erection processes.

On the other hand, taking into account wind effects in the selection of a tower crane model and configurations is challenging from a project management perspective. Furthermore, few number of studies have integrated tower crane capacity (which influence significantly the construction site productivity and total cost) as a factor in tower crane site layout optimization (TCSLP), since selecting the tower crane model was not within these studies scope. TCSLP is known as the problem of defining the tower crane location and the corresponding material supply locations. Previous studies investigated tower crane operations (i) did not integrate wind as an essential parameter in the process of tower crane model selection. (ii) developed algorithms for selecting the optimal design for the fixed anchorage type of the foundation of tower crane and overlooked the ballast base mode. (iii) did not present more than one solution according to decision makers preferences regarding the tower crane site layout optimization. In this context, the present study proposes: (i) a novel procedure for solving the site layout optimization problem in manner which reduces the time required and mitigates the extensive data manipulation involved through (ii) defining the tower crane location. (ii) selecting material supply locations. (iii) facilitating the tower crane model selection by presenting the critical weight and radius. Following to the crane model selection, (iv) a static wind analysis is applied to elevate safety precautions at the planning phase through. (v) examining the tower crane model capability to resist overturning and selecting the ideal ballast base dimensions and (vi) investigating the tower crane mast potential deformation and comparing it with safety consensus to guarantee the survival of the tower crane during extreme

5

wind speeds conditions. The developed methodology is presented as a computer software that maximizes applicability and minimizes pre-planning construction phase time.

Fig 2. Tower Crane Failure Republished from https://www.structuremag.org

Chapter 2: Literature Review

2.1 State of Art for Crane Type and Location Selection

Selection of crane types and their corresponding locations has been an area of interest to many researchers because it requires determining and evaluating of a large number of crane configurations [44] Knowing that, if crane selection and configuration are not done correctly, it may lead to cost, time and safety implications [45].

Warszawski [46] examined two expert systems, Locrane and Cranes, applied them to the crane selection and location problem, evaluated them and came to some conclusions with respect to the general applicability of expert systems to construction planning. Hornaday et al. [47] investigated a heavy-lift planning method, and presented a computer software program, HeLPS, that enables planners to evaluate hundreds of crane configurations through visualizing the execution of the heavy lift. Additionally, algorithms that determine the minimum lift radius have been integrated with computer-based CAD software packages (e.g., MicroStation) and database software (e.g., Oracle). Information pertaining to the lifted object (e.g., weight, dimensions), crane configurations (e.g., capacity, boom length) and the site characteristics are considered as inputs. Based on the inputs, the lift planner can select the suitable crane and for each configuration, the automated system provides possible locations. Afterwards, a crane location is selected based on the lift planner output. Finally, a lift path is automatically generated.

Hanna and Lotfallah [30] have used fuzzy logic to categorize all possible types of cranes based on their fitness value. Their designed system assigns fuzzy set values for each possible crane; for example, if a crane scored the value [0 0 0 0 0 0 0.2 0.4 0.6 0.8 1] then it is categorized as "good". They classified factors that affect the selection of crane type into (i) static, which is constant and doesn't depend on the nature of the project (e.g., cost of rent, mantling, and dismantling of the crane); or (ii) dynamic, which depends on the project (e.g., operating clearance and building height). All factors were given fuzzy set values representing the capability for every crane type (mobile crane, tower crane or derrick crane), then aggregated the data to come up with the best possible crane type.

Al-Hussein et al. [44] built an expert system called D-CRANE for crane selection to overcome the lack of support of the previously developed systems. D-CRANE is a comprehensive

database providing information about crane configurations, their lift capacity settings, and rigging equipment. Implementing a series of what-if scenarios, D-CRANE supersedes the traditional and limited use of load capacity charts and enables users to perform instant evaluations by giving a range of feasible solutions and alternatives that add flexibility in making the decision with more than 100,000 available crane lifting settings. D-CRANE incorporates a crane geometry algorithm with a schema of the database designed to focus on the development of an entity relational (ER) diagram. Moreover, Al-Hussein et al. [48] developed the mathematical model for the crane geometry. This model follows a four-steps process: 1) determine the crane lift capacity; 2) determine the crane's ability to fit on-site; 3) determine the boom and jib clearance with adjacent buildings; and 4) determine the lift itself. The four criteria must be satisfied for each lift setting retrieved from the crane database to confirm the technical feasibility. The output consists of a list of technical feasibility crane settings for lifts.

Sawhney and Mund [32] also utilized a knowledge-based expert system (KBES) with advanced artificial intelligence computing tools such as neural network-based system (ANN) in a computer software program called IntelliCrane. The software combines the two major modules with an interface and a database that contains a series of examples of crane types that were previously selected and considered as successful scenarios. Cases where the crane was considered to have a major effect on the construction project were also integrated. They used ANN to address problems where solutions are not clearly formulated or the relationships between inputs and outputs are vague. IntelliCrane made 313 correct crane type selections out of 340 cases with a success rate of 92.1%. ANNs, which are the cornerstone of this software, presuppose the availabilities of adequate training cases data for all types of cranes. For that reason, most errors were found to be in selections involving crawler-mounted hydraulic boom cranes and carrier-

mounted lattice boom cranes; crane types with insufficient data available. Another limitation is the inability to select more than one crane for a given construction site simultaneously.

Al-Hussein et al. [31] enhanced their model [44], and complemented their mathematical model for selection and location of mobile cranes on construction sites with an algorithm named Algorithm-1 that was then applied in their expert system D-CRANE by developing series of non-linear trigonometry equations (Algorithm-2) representing the material characteristics of the crane lift and site. MS-Solver was used for developing the optimization module due to the complexity of the equations. Different than Algorithm-1, Algorithm-2 is not constrained by predefined crane configurations and offers more flexibility for choosing lifting radii and boom lengths taken into consideration the minimum and maximum values mentioned in the manufacturer's capacity chart. They considered three scenarios: two for lattice boom with luffing jib when the main boom tip is higher or lower than the building height (lifting radii optimization is available), and one for hydraulic mobile crane (lifting radii and boom length optimization are available).

Tantisevi and Akinci [49] aimed to determine possible locations for mobile cranes with minimal relocation and to operate without running into spatial conflicts in any of the three dimensions. Previous related studies relied on 2D work envelopes, which can result in conflict and also in missing feasible probable crane locations. Implementing C++ programming language with OpenGL libraries for graphic visualization, they developed a prototype of an approach that visualizes and does a discrete-event simulation of crane processes based on dynamic crane behavior. To overcome the time-consuming simulation caused by investigating all possible conflicts at every single location and the existence of large quantities of objects lifted by cranes, this approach starts by checking crane reachability, which was previously approached by several researchers. After that, a boom-line intersection detection is performed to eliminate unfeasible

9

crane locations. Finally, expected crane motions are modeled and intersections of locations of cranes where conflicts can lead to collisions with surrounding buildings are detected. To minimize the relocation, the algorithm traverses backwardly and checks the crane location after the three tests, and if it was used for a preforming previous lift process, then the three tests are implemented again and a recheck is done. If this is the first operation in the sequence for this particular crane location, the latter is eliminated. Relocations are necessary when all locations are eliminated.

Wu et al. [50] built an algorithm represented in a systematic computer system for selecting lattice mobile cranes. This system integrates 3D-simulation, a rigging calculation module, and a database of mobile cranes with lift capacities varying from 50 to 1600 tons. The algorithm guarantees a lift setting's feasibility through a filtration process consisting of three lifting configurations. If any crane from the database does not satisfy the three tests, it is excluded automatically, and no crane configuration comes out to the user. The three tests are the crane's lifting capacity, clearances between boom/jib and the load, and the ground bearing pressure, which is ignored in most of the previous studies.

Hermann et al. [51] developed an approach to select crane types and locations, and also to simulate and schedule the lifting study plan using a database that contains crane dimensions and configurations. The approach outputs the study lifting plan in a 3D CAD model then visualizes it in a 4D animation for effective project execution using Navisworks.

Safouhi et al. [52] presented a mathematical algorithm for defining a mobile crane's bodywork area (MCBWA). The authors reduced the analysis time of crane positioning by performing a buffering function that uses inside boundary limits (ISBL) for objects inside the construction site and outside boundary limits for the entire site construction (OSBL) before checking capacity radius, boom clearance, and tailswing. This algorithm generates contours

10

outside the ISBLs, inside the construction site and inside the OSBL with an offset. This offset equals the minimum distance between the crane's center of rotation, any obstruction, and each side of the boundary limit for the construction site. An overlap algorithm is applied to combine the ISBLs and OSBL to result in the feasible mobile crane position area (FMCPA).

Olearcyzk et al. [53] proposed an approach for the crane selection process based on mathematical algorithms that were integrated with graphical 4D simulation for three stages. Crane load, capacity check, crane location, and boom and superlift clearance were taken into consideration in addition to factors such as lifted object size, lift procedure and weather restrictions. A case study, which involved the construction of five three-storey dormitories in 10 working days for Muhlenberg College in Allentown, Pennsylvania, resulted in a reduction in the duration of lift-planning by more than 50%.

2.2 State of Art of Safety and Wind effects on Tower Cranes

A troubling number of catastrophic crane collapses still occur in spite of all of the precautions taken by practitioners and project managers to ensure safety protocols are implemented on construction sites. Swuste [7] investigated a tower crane collapse at a Rotterdam building site on July 10th, 2008 in the Netherlands that was classified as a 'normal accident'. Results demonstrated that excessive inclination of the jib tested other components of the crane to the limit since the load was racked beyond the maximum load moment. Tort liability for the failure was not only due to an operating error but also due to errors in the crane design. Another incident involved a tower crane that was designed by the same manufacturer where the tower crane trolley was found to move too far, which verifies the crane manufacturer's responsibility [7] .

In China, Zhao et al. [9] made use of a fishbone diagram to introduce a hierarchical

quantitative analysis classifying the categories and causes of tower crane accidents. Tower crane tipping represented 53.3% of causes of accidents. In India, similarly, Sarkar and Shah [10] ranked environmental factors as the highest effective factor causing tower crane collapses. Tam and Fung [23] found that human factors such as improper training and indolent performance of tasks of practitioners is a major cause of safety violations. A Five-Point Likert scale was adopted by Tam and Fung [23] for conducting a survey questionnaire and structured interviews with crane operators, safety offices, and other crew members on construction sites. This questionnaire was designed to identify factors affecting safety in tower crane operations and to understand how the statutory requirements and non-statutory guidelines for the use of tower cranes were executed.

Zhou et al. [8] aimed to present a holistic hierarchical framework of contributing factors affecting tower crane safety from a complex sociotechnical system perspective through implementing analysis methods qualitatively and quantitatively. AcciMap model was built to present, in a comprehensive manner, the relationships and interactions among 56 factors that were considered from regulatory bodies (e.g., government safety regulations). Sorokin et al. [54] developed a neural network to forecast the wind gust speed and direction to ensure the stability of the tower crane against overturning. Li et al. [21] developed a multiuser virtual safety training system (MVSTS) to provide a totally risk-free and reasonable-cost environment for those involved in tower crane dismantlement process. An existing game engine (Virtools) was used to design this simulator. A scoring system recorded the incidents performed by trainees and dismantling processes were categorized into major mistakes (i.e., trainees fail their training if they make one these mistakes) and minor mistakes (i.e., trainees fail their training if they make two mistakes). The multiuser functionality allowed trainees to use the system simultaneously and different roles are available depending on the type of trainee (e.g., crane operator, safety officer). Moreover, the

MVSTS allows users to identify their own weaknesses and areas in which further training is needed, which is not possible with the traditional training process.

Beavers et al. [22] proposed that the Occupational Safety and Health Administration (OSHA) should emphasize more intervention strategies to facilitate investigations by researchers related to crane fatalities. The researchers pointed out that laborers working around a crane's working area must go through safety training as a result of their findings that most workers who die from crane-related events are not crane operators, rather they are specialty trade workers, e.g., laborers. Another recommendation was that crane operators and riggers should be requalified every three years. Shapira et al. [20] introduced a tower-crane mounted live video system to overcome several operational obstacles related to the operator's vision in spite of the top-of-the-crane cab location and its bird's eye view. Five scenarios were investigated, and the system improved not only safety issues, but also other influencing parameters for tower crane operations, such as productivity, direct cost, and ergonomics, were positively affected.

In Hong Kong, Lee et al. [19] developed a robotic luffing and saddle tower-crane system integrated with a laser-technology-based system to track the lifting-path of the lifted object in the context of improving safety. This system consists of two laser devices: one is to measure distance to the trolley and is connected to the intersection of the jib and the mast, the other measures the vertical distance to the rotation-controlled hook block and is connected to the trolley, and an encoder and an accelerometer measure horizontal and vertical angles. An adjustment algorithm was developed to overcome wind effect on swinging the lifted object. The laser system was preferred over other systems (e.g., GPS, machine vision) because of the cost effectiveness and accuracy.

Thirty percent of highway projects in the U.S. are conducted at night. Therefore, Hwang

[17] incorporated ultra-wideband (UWB) technology with collision-investigating prevention approaches to build a system that could monitor tower crane operations and asses the possibility of collision. UWB was favored due its high accuracy, which is accurate to within approximately 20 cm, it is not influenced by sunlight, and it is lower cost compared to data acquisition technologies such as radio frequency identification (RFID), global positioning system (GPS), and ultrasound. Moreover, the developed technology could cover an area of 400 m × 400 m. Tags were used to detect locations of tower crane booms and was paired to calculate the distances between booms of different of tower cranes for the system to be able to visualize the movement of booms in a simplified 2D environment and to warn the operator if there exists any potential for collision.

Li and Liu [18] created a data-driven remote monitoring and alarm system for guaranteeing safer tower crane operations. Their system depends on a "plug and play" data (e.g., tower height, lifting load, slewing speed) acquisition system represented by controller area network (CAN). The system applies a kinematic analysis using module-position-attitude-scale (MPAS) for virtual crane activities that are acquired by field sensor data and warns of the potential accidents presented in a real-time 3D simulation system which evaluates the operation safety. Shin [11] discovered that 64% of all fatal accidents involving tower cranes in South Korea happened during installation and dismantling. Consequently, he focused on identifying the main causes of those accidents to develop more effective regulations for guaranteeing safe operations.

Wind is volatile and unpredictable. When it comes to crane failures due to excessive wind speed, these can be difficult to predict, especially if the cause is wind gusts (which can occur unexpectedly). Many researchers have explored the ramifications of wind on tower and mobile cranes. For instance, Klinger [55] explored two crane accidents focusing on analyzing manufacturing material, where fatigue cracks and surface fractures were observed. Ross et al. [56],

calculated the wind loads and performed structural and stability analyses for the Miller Park accident in order to determine whether the tort liability fell to the crane designer or the contractor. Chen et al. [57] applied computational fluid dynamics to determine the most unfavorable wind load direction, concluding that "cross-wind" loads should be considered along in addition to "along-wind" loads in terms of tower crane design. Using finite element analysis (FEA), El Ouni et al. [58] attempted to mitigate turbulent wind excitation on the tower crane vibrations by deploying an active damping system. Mara [59] studied the aerodynamics variations excited resulting from bracing a tower crane to a high-rise building, implementing wind tunnel tests. They found that, the tower crane's presence in the vicinity of a building, specially, if closer to the building's corner, amplifies the base torsion moment nonetheless, a tower crane location closer to the center of the building alleviates the moment. Voisin et al. [60] conducted wind tunnel tests on scaled tower crane models to study their out-of-service behavior. They observed that wind moments showed a higher likelihood to overturn the tower crane compared to inertial and centrifugal moments. Jiang and Li [61] applied features of the finite element analysis to explore the wind-induced dynamic reliability of a tower crane structure by estimating the vibration strength and horizontal displacement occurred within different winds speeds and directions.

2.3 Tower Crane Site Layout Optimization State of Art

Tower crane site layout optimization (TCSLP), due to its complexity, has been extensively evaluated. Leung and Tam [62] examined the ability to predict tower cranes hoisting times using multiple regression models (MR) for supply and return hoist times. This model was shown to aid the planners in forecasting any changes in overtime requirements in hoisting times for different locations. Twelve factors were considered in this study (e.g., angular and radial movement, the

weight of the load and hoisting height), and hoisting height was found to be the most impactful factor on hoisting time. Similarly, Tam et al. [63] attempted to predict tower crane hoisting times using two types of nonlinear neural networks, GRNN and GMDH. Moreover, they compared the performance of general regression neural network (GRNN), group method of data handling (GMDH) and multiple regression (MR) in terms of robustness, accuracy, and reflection of relationships between input variables.

Zhang et al. [64] presented a mathematical model which can approximately determine the cycle time of a tower crane. Their study used Monte Carlo simulation to delineate a single tower crane location optimization. Zhang et al. [65] addressed the case of multiple tower cranes with the aim of balancing workload and identifying spatial conflict. However, supply point locations were not within their scope. Tam et al. [66], relied on computational optimization to handle SLP nondeterministic polynomial intricacy using Genetic Algorithms (GA) specifically for determining tower crane and supply points locations. They used total cost of the tower crane workload as the GA fitness value. Furthermore, they provided travelling speeds and the cost of operating a tower crane per minute, subsequently adopting these values in their case study to compare its effectiveness against existing optimization techniques available in the literature.

Tam and Tong [67] integrated ANN and GA, training the former using the software NeuroShell for modeling the non-linear nature of operations of the tower crane and normalizing project-specific parameters such as height of high-rise building model, while the latter was employed for optimizing the tower crane and supply locations.

Despite the majority of prior studies offering methodologies that provide objective, quantitative and scientific ways to evaluate the effectiveness of a particular site layout in the context of crane placement, the methodologies encountered limitations in dealing with large

16

construction areas. In the case of that particular predicament, Alkriz and Mangin [68] demonstrated two formulations of genetic algorithm (GA), of which one of them was designed specifically for large construction sites. The authors claimed that a 31% reduction was achievable in terms of tower crane cost and time compared to the original plan. Huang et al. [69] using LINGO software, applied a mixed-integer-linear programming (MILP) and found it to be 7% more efficient compared with GA for modeling the crane and supply layout from material transportation frame of reference. For the purpose of the comparison, it should be noted, they used two cases considering homogenous and non-homogenous supply points. Moreover, they added a numerical parameter to capture the inherent challenges of site operation and their effect on crane's operational time. Later, Huang and Wong [33] applied BMILP, finding that, it surpassed the performance of traditional scheduling algorithms such as first-in-first-serve (FIFS), shortest-job-first (SJF), nearest-neighbor-first (NNF) and Traveling salesman problem (TSP) for solving more complex practical operational problems involving tower cranes. Additionally, they prioritized urgent material demand requests and embedded the hook start point position per the Zhang et al. [65] model, in addition to modifying the hook vertical movement equations. Similarly, Lien and Cheng considering material transportation, juxtaposed the efficiency of Honey bee (HB), Bird Swarms (BS) and Particle Bee algorithms (PBA); a proposed algorithm integrating the advantages of the two aforementioned algorithms resulted in a best mean fitness value to minimize the operating cost. They also took into account the total rent cost and setup of the tower crane.

In the context of the tower crane site layout optimization problem (TCSLP), Abdelmegid et al. [70] proposed to include the number of cycles required for each building zone depending on the handled material quantity. Furthermore, they examined the hook vertical travel time and subcategorized it based on the speed, which will vary depending on whether the hook is loaded or

unloaded. Huang et al. [71] demonstrated the existence of a linear correlation between the precast rate and the total cost for tower crane operations and their effect on the crane's selected type and location. Tubaileh [72], utilizing a simulated annealing (SA) algorithm, approached the TCSLP differently with a robotic perspective considering continuous variations in the hoisting velocities. Conceptually, he presented a cubic spline trajectory planning between two loading points for the crane emphasizing kinematic and dynamic constraints. Moreover, the relationship between the rated power of the electrical motors and lifting capacity was not eliminated as an additional constraint.

Hosseini et. al [73] designed a computer program to select the best place for crane erection and suitable crane type based on the minimum radius for the requested crane. Kaveh and Vazirina [74] adapted the case study by Huang et al. [69] and compared the performance of three optimization algorithms: colliding bodies optimization (CBO), enhanced colliding bodies optimization (ECBO), and vibrating particle (VPS). ECBO showed a more stable result than either VPS or CBO, except for the case of homogenous material site, which was slightly advantageous towards VPS, but none of the three algorithms presented better optimized cost than MILP. In Indonesia, Husin and Priyanto [75] applied lean construction concepts to optimize cost-time efficiency.

Monghaesmi et al. [76], based on game theory, least deviation method, power index method and harmony search (HS) algorithm novel-optimization, developed a hybrid approach to balance the waiting time for multiple tower crane operation requests versus order crane operation requests as an alternative to relying on hook travel time as the basis for operational planning. Briskorn and Dienstknecht [77] proved that limiting the infinite possibilities of a tower crane location to a finite set without losing the optimality is plausible. Consequently, the problem was

transformed to a classic weight set cover problem (WSCP) and solved via extensive computational study. Younes and Marzouk [78] using agent-based simulation (ABS) showed that luffing jib tower cranes are preferable to saddle jib tower cranes in terms of cost and safety due to their higher maneuverability. Using AnyLogic software, they presented a method for determining the optimum combination of tower cranes type, number, and locations by integrating the ABS model with the model proposed Zhang et al. [65] adding a numerical factor to capture the tower crane time when the latter is already operating but not properly used. Lee et al. [79] applied the harmony search (HS) algorithm for optimizing the locations of a single luffing jib tower crane and material supply. All the above-mentioned studies adapted the construction site layouts from a 2D perspective.

Irizarry and Karan [80] connected GIS and BIM for a 3D visual model. Crane locations were derived by the model and resulted in 3% more supply and demand points compared to those areas included in the operating area for tower cranes located on an actual site and a 16% reduction of conflict index. Even though the developed method suffers from interoperability between GIS and BIM, it needs a user who has prior knowledge pertaining to exchanging data between the two. Al-Hussein et al. [36] presented SimAnim, a powerful tool that bridges the gap between discrete event simulation and real-world visualization of tower cranes construction operations. Wang et al. [42] utilized the firefly algorithm (FA) in conjunction with building information modeling (BIM) in order to demonstrate a 4D-BIM tower crane layout plan from the operator's perspective. Their proposed layout plan allows the operator to detect collisions as well as confirm coordinates, activities, and installation, and simulate climbing and demolition of the tower crane. Marzouk and Abubakr [81] proposed a decision support framework that integrates BIM and GA to present a 4D site layout model equipped with a tool to mitigate risk of conflicts and includes types, number, allocations and lifting schedule of tower cranes. They argued that a lower capacity tower crane

leads to a lower rental cost and can considerably lower the overall costs of the lifting operations. Building on this hypothesis, Nadoushani et al. [82] and, Ji and Leite [83] expanded on the MILP model proposed by Huang et al. [69] The study by Nadoushani et al. described tower crane location as a site-layout-specific condition and explored its impact on the desired capacity and, thus, the total cost. Notably, they created a list of various potential crane models categorized by capacity, rental cost, and operating costs in order to support selection of the model that minimizes that overall cost. The study by Ji and Leite [83] , meanwhile, adapted the same approach for multiple tower cranes.

Table 1 classifies the site layout literature based on the criteria considered in each given publication.

Table 1 Site Layout Literature Review classification

Paper	Tower Crane							Dimensionality			Resource Allocation				Material Handling		Research objective and Method adopted, Contribution
	Single	Multiple	Balanced Workload	No of cranes	Collision detect	Luffing crane	Location	2D	3D	4D	limited	Unlimited	Urgent	Non-Urgent	Location-assign	Non-Assigning	
Leung and Tam [62]	x							x									Mathematical regression model for predicting hoisting time
Tam et al. [63]	x							x									Compare GRNN, GMDH and Multiple regression efficiency to predict hoisting times
Zhang et al. [64]	x						x	x									C++ code processed a mathematical model for predicting hoisting time
Zhang et al. [65]		x	x		x			x								x	Mathematical model for predicting hoisting time

Reference													Notes
Tam et al. [66]	x				x	x		x		x		x	Genetic Algorithm for predicting hoisting time, literature travel speeds and operation cost/min
Tam et al. [67]	x				x	x		x		x		x	Genetic Algorithm and Neural Network for minimizing total cost
Alkriz and Mangin [68]		x	x	x	x			x		x		x	Genetic Algorithm for large construction sites
Huang et al. [69]	x				x	x	x	x		x	x		MILP is compared with GA for optimizing the tower crane site layout with min. cost
Huang et al. [33]	x				x	x	x	x	x	x	x		BMILP is compared to FIFS, STF, NNF and TSP for optimizing the site layout with min. cost, Numerical Parameter reflect crane location difficulties
Lien and Chang [84]	x				x	x		x		x	x		PBA is compared to HB, SBI for optimizing site layout, embedding dismantling and mantling cost
Abdelmegid [70]	x				x	x		x		x		x	GA for optimizing the site layout location with min. cost, Number of load cycles, load and unload vertical speeds, area constraint for overlaps between crane and supply locations
Tubaileh [72]	x				x	x		x		x	x		Simulated Annealing Algorithm with NAG toolbox, considered velocities variations and relationship between electric motors rated power and the crane capacity
Hosseini et. al [73]	x				x	x		x		x		x	Mathematical model for minimizing the tower crane operation cost through minimizing the lifting radius
Kaveh and Vazirinia [74]	x				x	x	x	x		x	x		Compare ECBO, CBO, VPS performance for optimizing site layout through minimizing cost
Trevino and Abdel-Raheem [85]	x				x	x							ACO for single tower crane allocation, mentioned the swing angle equation flaw
Monghaesmi et al. [26]		x			x	x					x		Game Theory, least deviation method and HS algorithm to balance and minimize tower cranes

														waiting time and order sequencing
Briskorn and Dienstknecht [27]		x					x	x			x		x		x	Converting the tower crane site layout problem to a classic weight set cover problem, limiting infinite number of locations to a set without losing optimality
Marzouk and Abubakr [81]		x	x	x	x		x			x					AHP, sensitivity analysis and genetic algorithm to select crane type, determine number of tower crane and visualize the lifting schedule
Younes and Marzouk [78]		x	x	x	x	x	x	x							Agent based Modeling for optimizing site layout through minimizing operating time and cost
Lee et al. [29]	x					x	x	x							Heuristic approach and Harmony Research to determine the luffing tower crane location through minimizing operating time
Irizarry and Karan [30]		x	x		x		x		x		x	x			Interconnection of GIS and BIM for a 3D visual model of tower crane site layout optimization
Wang et al. [32]		x	x	x	x		x			x	x	x			Firefly Algorithm (FA) utilization with (BIM) to simulate and confirm the crane activities
Nadoushani et al. [82]	x					x	x			x	x		x		MILP to optimize tower crane layout embedding crane capacity prior to optimization by minimizing total cost
Ji and Lietie [83]		x	x			x	x			x	x		x		MILP integrating crane capacity for multiple tower cranes site layout optimization

Prior studies that investigated the effect of wind on tower cranes structures and studies incorporated crane capacity into tower crane site layout optimization (i) analyzed the immediate causes of accidents or the relationship between wind and tower crane location. (ii) proposed solutions for mitigating wind reverberations regardless of wind effect as a decision-making component in the selection of tower crane models and configurations. (iii) have been specific-

project analyses requiring expertise in 3D modeling and computational fluid dynamics. (iv) presented only one optimal solution neglecting decision makers' preference to seek faster crane operations (changing the material supply locations) due to tight schedules and deadlines (v) assigning a material supply location for each demand location [82], where it has been for the user to assign manually each demand location a supply location.

To overcome those limitations, this paper proposes a decision support tool for tower crane model selection and site layout optimization as outlined below.

1. Regarding tower crane site layout optimization, a twofold mathematical optimization approach that seeks to minimize the operation time needed for the crane motions to be performed and reduce the momentum generated around the crane base is proposed in order to facilitate selecting the tower crane model and determine the most feasible crane location and the designated supply location for each demand location

2. Regarding tower crane model selection, a simplistic static analysis-based decision support framework is developed to ensure the adequacy of the selected tower crane model buffeted by high wind speeds. Wind speeds can lead to reverberation, overturning, and mast structural beam failure due to excessive malformation. Specifications such as ground bearing pressure and allowable limit of deflection of the tower crane are, respectively, the measures for the resistance of the tower crane against extreme weather conditions. It is worth mentioning that, the tower crane is assumed to be a rigid body and dynamic forces repercussions were not included.

.

Chapter 3: Methodology

Fig 3 illustrates the proposed methodology, which consists of two primary frameworks interconnected to assist decision makers with increasing the productivity and safety of tower crane operations. The first framework assists practitioners with selecting the optimum crane location and supply locations from which to transport material. This process minimizes the effect of tower crane operation time and crane capacity as parameters in devising the layout of the construction site. The key parameters that need to be provided in order to initiate the process include, the potential location (geographic coordinates) of the construction project, the weights and dimensions of the payloads, the number of floors to be constructed, and the diameter of the unoccupied area required to maintain the clearance around the tower crane base to avert collisions. The TCSLP framework, then, checks the data compatibility before initiating the calculation of all potential lifting moments (supply and demand locations moments) for all inputted locations. The TCLSP framework, then, mathematically optimizes the lifting moments of prospective crane and material supply locations and demand locations and unifies each pair of moments values into one value as classifying weight based on a distance-based optimization technique. (bearing in mind that the lifting moment mirrors the crane capacity). Following this, the TCSLP framework estimates the amount of time expended transporting the modules, investigating all potential locations following the mathematical model of Zhang et al. [65] to determine the horizontal, vertical and thereby the total time of moving a payload between the crane, supply and demand locations. Finally, a twofold mathematical optimization combining the lifting moments optimization and hook travel time modeling is applied using distance-based optimization technique. The optimization aims to select the optimum crane and supply locations contingent upon the user's preference between a more conservative crane operations (and, therefore, lower total cost) versus a tighter crane operation schedule. Inclining to more conservative operations drives the algorithm to select closer and a smaller number of supply

locations to the crane location therefore, minimizing possibility of exerting higher lifting moments on the tower crane. In contrast, faster crane operations increases the Euclidean distance in between crane and supply location and decreases the distance in between supply and demand locations. Moreover, the different velocities of different tower crane models (slower slewing velocity) might lead the algorithm to choose further crane locations from the demand locations within the available provided locations to reduce slewing angles.

The program generates a list of supply locations assigned for each demand location, a 2D scatterplot for better visualization for the site layout, detailed information related to each lift operation time, total cost of the lifting operations, critical weight and lifting radius. The two latter outputs are employed to select the tower crane model and advance to the second framework (wind resistance framework), which tests the ability of the tower crane model to withstand extreme wind gusts (where a failure may be in the form of overturning or over-limit mast deflection). Information such as maximum potential wind gust, the surrounding environment (e.g., urban versus rural), tower crane configurations, initial ballast base dimensions for anchoring the tower crane, and dimensions of critical weight and radius serve as the input data for the static mathematical model applied for the tower crane model investigation. Based on the mathematical model, the wind resistance framework evaluates tipping over wind moments (over the rear and over the sides moments) which are induced from wind gust pressure on the tower crane structure. At first, the support legs reactions are defined through calculations of ground bearing pressures. Ultimately, the wind resistance framework, identifies whether the ballast base dimensions are sufficient to prevent overturning with a 360° plot for the four tower crane leg reactions, and assesses how they react with different tower crane swinging angles. At second, the wind resistance framework using same calculations were applied before the calculation of the leg supports, to calculate the deflection

of the tower crane mast. Tower crane elements' moments over the tower crane base weights and their distance from the tower crane center of gravity (CG) are imperative to be calculated.
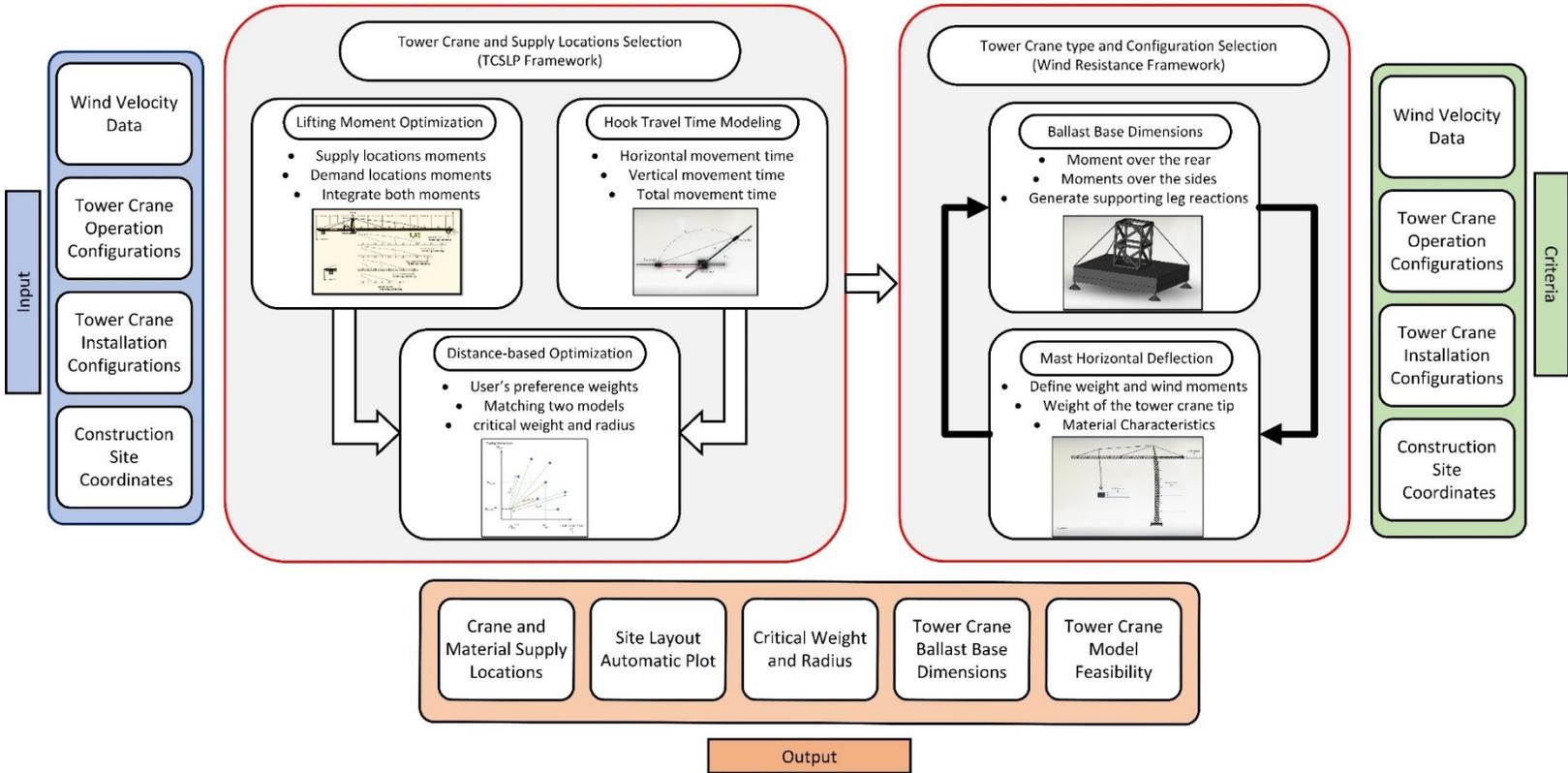
Fig 3. The Proposed Methodology

3.1 Site Layout Optimization and Tower Crane Model Selection

3.1.1 Lifting Moments Mathematical Optimization

The first phase of the presented study seeks to enhance preconstruction phase planning. The proposed algorithm aims to present more efficient tower crane operations and configurations. This is achievable through, determining the tower crane capacity, location, and the supply locations by giving to the practitioner a percentile weight ratio which can be used as the basis for selecting

between leaning for minimizing the time expended for the tower crane hook movement or safety improvement by mitigating the base-load moment. The lifting moment, it should be noted, is what induces the propensity of rotation around an axis; excessive moments values are thus hazardous for tower cranes. In this context, the purpose of this section of the methodology is to mitigate the lifting moments and thereby avoid a costly overdesign by selecting the crane with right capacity. A generic approach is developed to better understand the effect of the crane capacity on the output of the methodology. For the optimal functionality of this model, the following assumptions are considered:

- Candidate crane locations supply points coordinates are predetermined with an infinite storage capacity for the latter.

- Demand modules information (i.e., location, weight, dimensions) is predefined and each demand location is assigned to only one source point location.

- Material type is not part of the site layout optimization.

- The single selected tower crane is capable of providing full coverage within its permissible lifting radius and capacity to the total number of the demand locations.

- All the aforementioned data is provided in the format of an MS-Office Excel (.xlsx) file.

Site layout optimization has always been classified from a computational complexity theory standpoint as a non-deterministic polynomial-time (NP) hardness problem [69]. In other words, there is no algorithm with polynomial time capable of achieving the optimum result. As a result, knowledge base methods, approximate mathematical approaches, and general heuristics have been developed to generate (near-) optimal solutions. Nevertheless, it is the meta-heuristic methods that has been adopted by the majority of researchers attempting to solve problems of this nature [86]. In the present study, a computer program is created in order to draw a solution which is closer to

optimality regarding the computational complexity. Building on the algorithm developed, a new implementation which integrates the time dimension to the tower crane operation has also been proposed [65,69]. Solving the site layout problem, it should be noted, necessitates four parameters as inputs for the algorithm: (i) potential crane locations, (ii) potential supply locations (iii) demand locations, and (iv) lifted module weights. Whether overlapping or segregated, the sets of areas where a crane can be anchored or from where material can be picked must be discretized into a set of points defined by their Cartesian coordinates $\{(x_k, y_k, z_k)\}_{k \in K}$ where k is a potential crane location within the set of crane locations K. That being said, the set area J is always predefined since they present the lifting operations destination; furthermore, the modules weights and demand locations numbers must be identical, as each weight has only one assigned demand location. The predefinition of the demand locations does not diminish their footprint on the site layout optimization to avoid driving the algorithm towards selecting a crane location closer to the supply locations without considering demand locations effect. Therefore, the crane location selection is a two degree of freedom (2DOF) problem connected to the optimization of supply and crane locations (supply moments and demand moments).

It should be noted, the calculation of the lifting moment M_{load} exerted by a payload is given as per Equation (1),

$$M_{load} = W_{load} * d \tag{1}$$

where the W_{load} is the weight of the payload with all the accessories (e.g. shackles, spreader bars, slings, hook, etc.) needed to perform the lift and d is Euclidean distance separating the center of mass of the payload and the center of the mast. In the absence of forces contributed by external

factors such as wind or load swinging, the rest of the lifting moment mathematical optimization can be described as per Equation (2),

$$\sqrt{M_{k,s,c}^2 + M_{k,d,c}^2} \quad k = 1, 2, \cdots N, \qquad (x_s, y_s) \in S, \quad (x_d, y_d) \in D, \qquad (x_c, y_c) \in C$$

$s.t.$

$$M_{k,s,c} = w_k \sqrt{(x_s - x_c)^2 + (y_s - y_o)^2} < M_{max} \quad k = 1,2, \cdots N \quad and \ (x_s, y_s)$$

$$\in S, (x_c, y_c) \in C$$

$$M_{k,d,c} = w_k \sqrt{(x_d - x_c)^2 + (y_d - y_c)^2} < M_{max} \quad k = 1,2, \cdots, N \quad and \ (x_d, y_d)$$

$$\in D, (x_c, y_c) \in C$$

$$C_1 \leq \sqrt{(x_s - x_c)^2 + (y_s - y_c)^2} \leq R_{k,s,c} \qquad (x_s, y_s) \in S, \qquad (x_c, y_c) \in C$$

$$C_2 \leq \sqrt{(x_d - x_c)^2 + (y_d - y_c)^2} \leq R_{k,d,c} \qquad (x_d, y_d) \in D, \qquad (x_c, y_c) \in C$$

(2)

Where w_k represent the weight of payload $k = 1,2, \cdots N$ and S, D and C are respectively the set of supply, demand and crane locations identified by their projected Cartesian coordinates (x, y) on the XY plane; the constants C_1 and C_2 represent the clearances between the crane mast and the payloads. As for the generic notation $R_{k,u,c}$ it refers to the reach of the crane for a payload w_k picked (or dropped) at a point defined by (x_u, y_u) by a crane located at (x_c, y_c).

From an implementation perspective, since the supply, demand and crane areas are discretized, as shown in Equation (3), determining an optimal solution can be obtained by means of nonlinear programming. However, when the size of the problem, i.e. $N \times |S| \times |D| \times |C|$ where $|A|$ is the cardinality of set A, lies within reasonable bounds, a brute force approach which starts by computing all possible moments before extracting optimal solution(s) may also be used. In

Equation (3), the objective function can be viewed as a search for the point defined by $(M_{k,s,c}, M_{k,d,c})$ that is the closest, in the sense of the Euclidean distance, from the origin. This choice was motivated by the fact that a supply point with a small moment $M_{k,s,c}$ can possibly be associated with a demand moment $M_{k,d,c}$ that is excessively high. Distance-based optimization is a heuristic approach widely used because of its computational efficiency. It classifies data non-probabilistically into a group of contributors and utilizes distances in between the elements as objective benchmarks for the purpose of identifying resemblance between different objects [88,89]. Conceptually, Euclidean distance is employed and mirrored through a weight assigned to each element representing the twofold moments for the corresponding crane, supply and demand locations. The implementation flow built upon Equation (3) is Fig 4
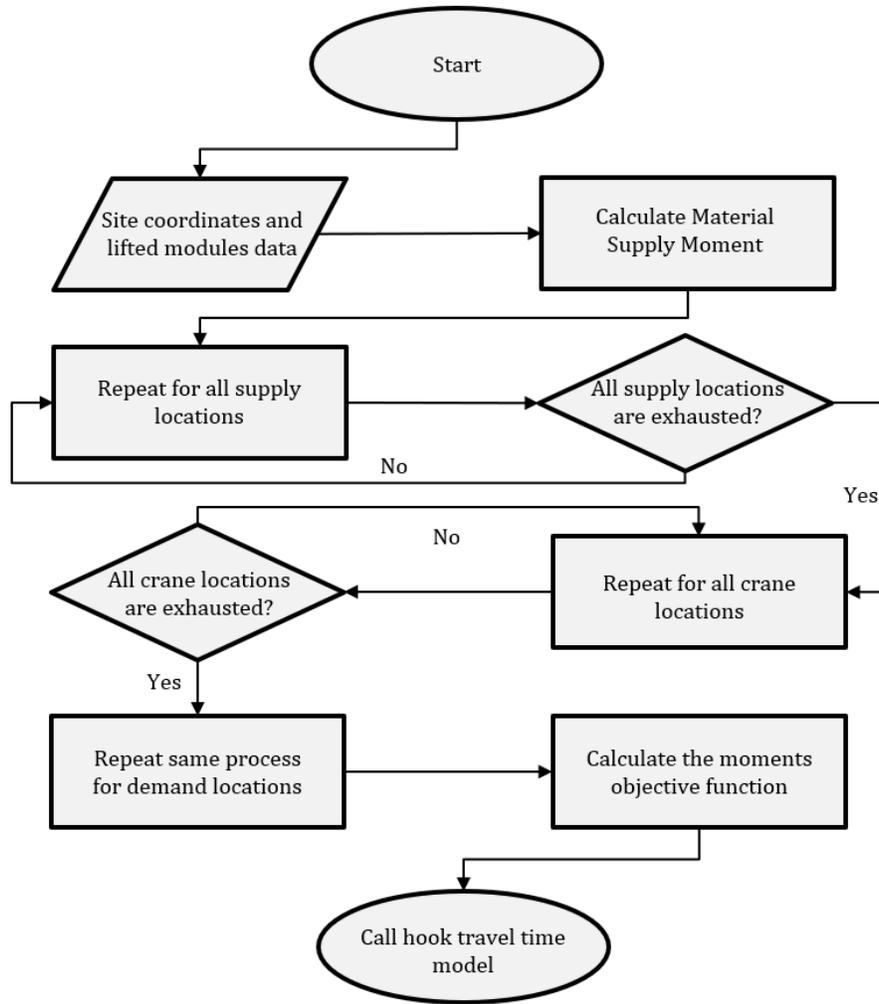
Fig 4. Flowchart of moment-based procedure for evaluating locations

3.1.2 Hook Operational Travel Time Mathematical Modeling

3.1.2.1 Model Explanation

For the purpose of calculating the hook travel time, the mathematical model proposed by Zhang et al [65] and augmented by Huang et al. [69] is adopted, where the same assumptions mentioned in the previous section are considered; the tower crane hook movement can thus be divided into three possible operations: transversal (also called trolleying), slewing, and vertical movement (also

called hoisting). Using the variables defined in Fig 5, the time needed to trolley between the supply

and demand radii, $T^r_{(s,d,c)}$ and to swing between these locations is defined by Equation (3) and (4)
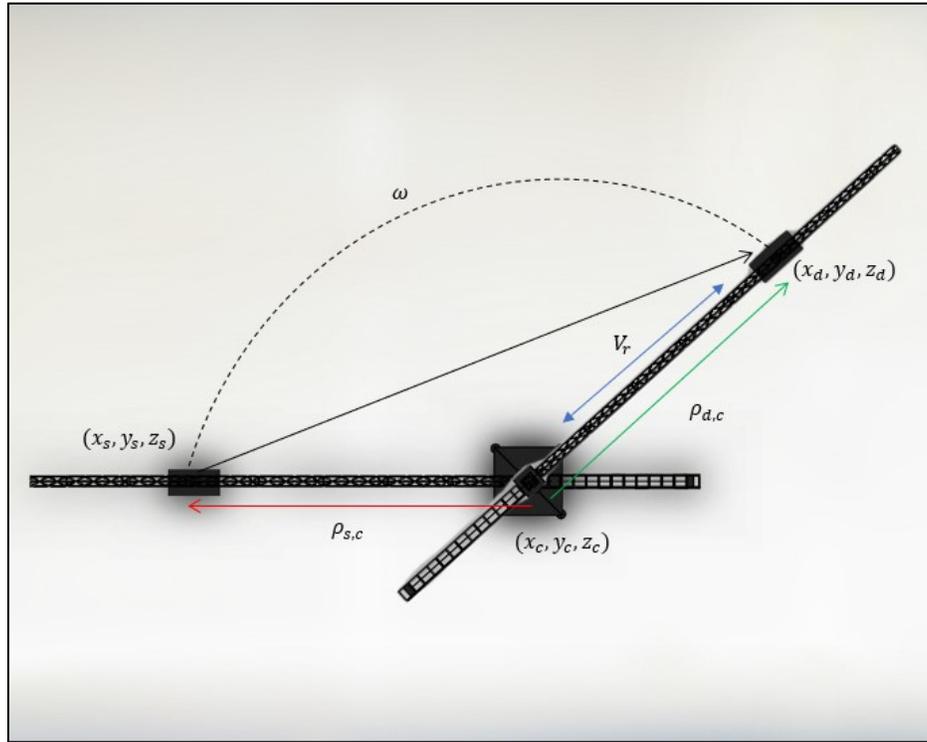
Fig 5. Tower crane slewing and transversal movement (horizontal movement) between crane,

supply, and demand locations

$$T^r_{(s,d,c)} = \frac{|\rho(d,c) - \rho(s,c)|}{V_r} \tag{3}$$

$$T^{\omega}_{(s,d,c)} = \frac{1}{V_{\omega}} \cdot arcos \left(\frac{[(x_s - x_c).(x_d - x_c) + (y_s - y_c).(y_d - y_c)]}{\left[\sqrt{(x_s - x_c)^2 + (y_s - y_c)^2} \cdot \sqrt{(x_d - x_c)^2 + (y_d - y_c)^2}\right]} \right) \tag{4}$$

Where V_r and V_{ω} are respectively the radial and angular velocities of the hook when trolleying and slewing (with the jib). Equation (4), is developed as replacement for the slewing trigonometric equation developed by Zhang et al. [65] in order to eliminate increasing of hook travel movement the latter produces since, it generates the reflex angle (> 180). This model is feasible for use in cases involving luffing-type tower cranes, with Equation (5) employed as an alternative to Equation (4) to address the translation of the object achieved by luffing up and down, which is, the main difference between luffing tower cranes and saddle tower cranes [87]. Where R is the length of luffing tower crane jib.

$$T^{L}_{(s,d,c)} = \frac{1}{V_{\omega}} \cdot arcos \left(\frac{Min(\rho(d,c),\ \rho(s,c))}{L_{luffing}} \right) - arcos \left(\frac{Max(\rho(d,c),\ \rho(s,c))}{L_{luffing}} \right) \tag{5}$$

The time exerted for the total horizontal movement can be predicted from Equation (6) which is an amalgamation of the jib trolley translational and jib radial movements where α is a parameter specifying the degree of coordination between both leaning on the tower crane's operator experience for coordination between the two types of movements. Values between 0 and 1 are recommended where 0 represents a full simultaneous movement and 1 mirrors full consecutive movement. Fig 5 is a demonstration for the horizontal movement.

$$T^h_{(s,d,c)} = max\left(T^r_{(s,d,c)}, T^\omega_{(s,d,c)}\right) + \alpha . min\left(T^r_{(s,d,c)}, T^\omega_{(s,d,c)}\right) \qquad (6)$$

The time associated hoisting (vertical) motion also needs to be valuated as per Equation (7), where $|z_i - z_j|$ represents the hoisting distance and V_h the hoisting velocity (see Fig 6).

$$T^v_{(s,d,c)} = \frac{|z_s - z_d|}{V_h} \qquad (7)$$
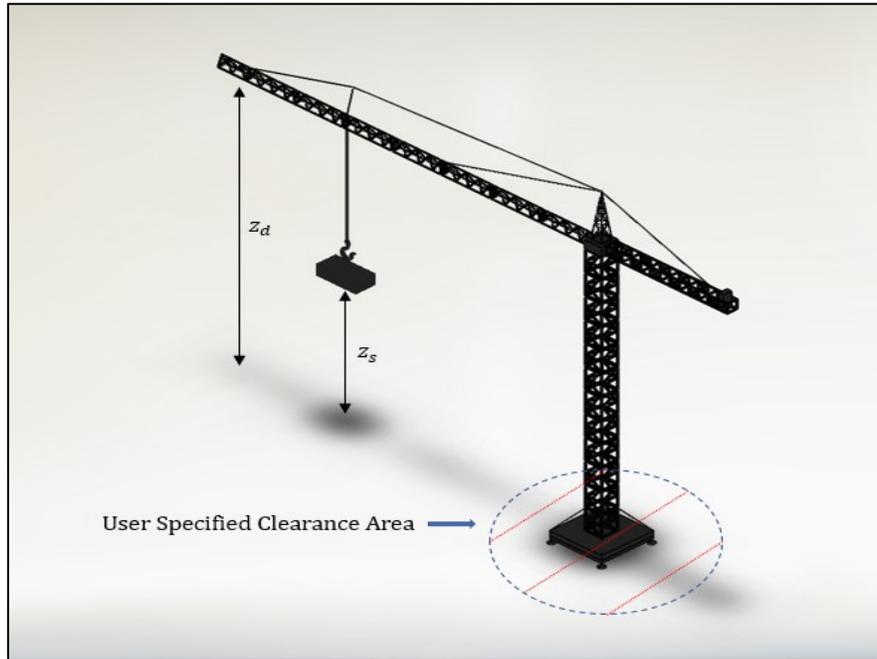
Fig 6. Tower crane's vertical movement between supply and demand location

Finally, to build a complete account of the time needed to operate a crane moving a payload between the supply and demand locations, the duration needed for horizontal motion, i.e. trolleying

and slewing, needs to be add to its vertical counterpart. However, since transitioning from one motion to another penalizes the continuity of the operation, the total time needs to be adjusted to account for these necessary interruptions. In this context, the total time is defined satisfying Equation (8), where β ($0 \leq \beta \leq 1$), similarly to α parameter, reflects the tower crane's operator experience for coordination between the two types of movements (horizontal and vertical movements) and γ_k ($1 \leq \gamma_k \leq 10$) is a function mirrors difficulty of obstructions to maneuver the crane hook at a crane location k.

$$T_{(s,d,c)} = \gamma_k \{ max(T^h_{(s,d,c)}, T^v_{(s,d,c)}) + \beta. min(T^h_{(s,d,c)}, T^k_{(s,d,c)}) \} \tag{8}$$

3.1.3 Twofold Mathematical Optimization

The majority of previous studies investigating the site layout problem have employed the mathematical algorithm proposed by Zhang et al. [65] for estimating tower crane hook operating time. However, as mentioned previously, few studies have integrated crane capacity as an intrinsic parameter as previously mentioned due to overshadowing the selection of the tower crane model, and in those only one solution was presented [82]. The computer program developed in the present research, in contrast, produces an optimized solution based on the user's preference. A tower crane with a higher capacity correlates to higher rental, operating, and maintenance costs, but sometimes preferable when the decision maker is on a tight schedule or already selected the tower crane model and under pressure to expedite operations. As previously mentioned, slower slewing velocities leads the algorithm to decrease the slewing movement therefore sometimes increase the Euclidean distance between different locations. In contrast and by default, the developed software is able to

optimize for both capacity and duration. In this respect, since crane capacity can impact its location and in turn the time needed to deliver payloads, an alternative objective function is devised in this work satisfying Equation (9) and as shown in Fig 7

$$min \sum_{k,s,d,c} \sqrt{p_m \cdot \left(\frac{M^o_{k,s,d,c} - min\, M^o_{k,s,d,c}}{max\, M^o_{k,s,d,c} - min\, M^o_{k,s,d,c}}\right)^2 + p_t \cdot \left(\frac{T_{k,s,d,c} - min\, T_{k,s,d,c}}{max\, T_{k,s,d,c} - min\, M^o_{k,s,d,c}}\right)^2} \qquad (9)$$

Where $M^o_{k,s,d,c}$ is the optimal value of the objective function given in Equation (3) and $T_{k,s,d,c}$ is the total duration to move payload k from supply point s to demand point d with a crane located at point c. As for the terms $0 \leq p_m \leq 1$ and $0 \leq p_t \leq 1$ they are defined by the practitioner depending on whether emphasis is put on having small moments or shortest operation times. Geometrically, the above objective function amounts to searching a point defined by the coordinates $\left(M^o_{k,s,d,c}, T_{k,s,d,c}\right)$ which is the closest, in the Euclidean sense, to an ideal point identified as $(0,0)$.

After the optimization based on Equation (9) which provides the supply locations and the crane, it is also important to include the cost dimension which includes the rental and operating cost parameters. Equation (10) sets the total cost procurement TC as a function of the total operating time and crane capacity where, C^m_o and C_R are the rental and operational costs, respectively, of a tower crane of type m. Fig 8 is a flowchart showing the procedure to implement twofold mathematical optimization. The output information—including optimal crane location, the assigned supply location for each module's final destination, the operation time for each process, the total operation time, the critical radius, the critical lifting moment, and the total cost—is saved

in a CSV file. Additionally, an automatic scatterplot of the site layout is generated depicting the

site coordinates as well as the allocated crane and supply locations.

$$TC = (C_R^m + C_o^m) \times T_{(i,j,k)} \tag{10}$$
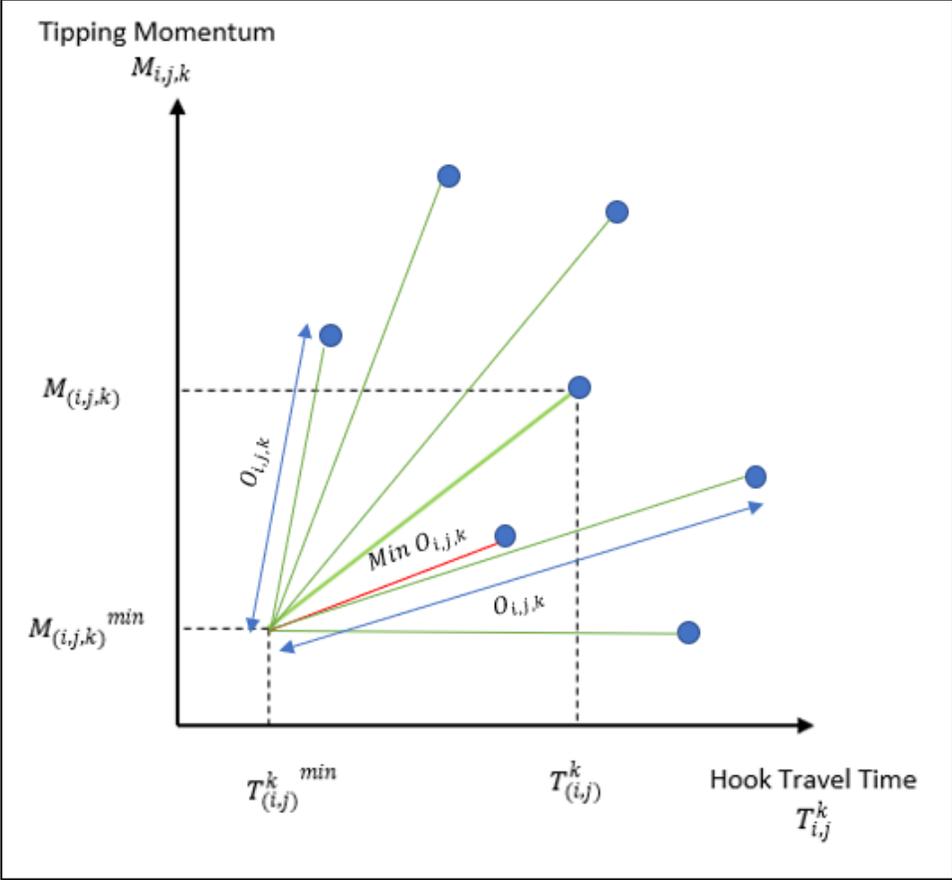
Fig 7. Optimization of tipping moment and hook travel time
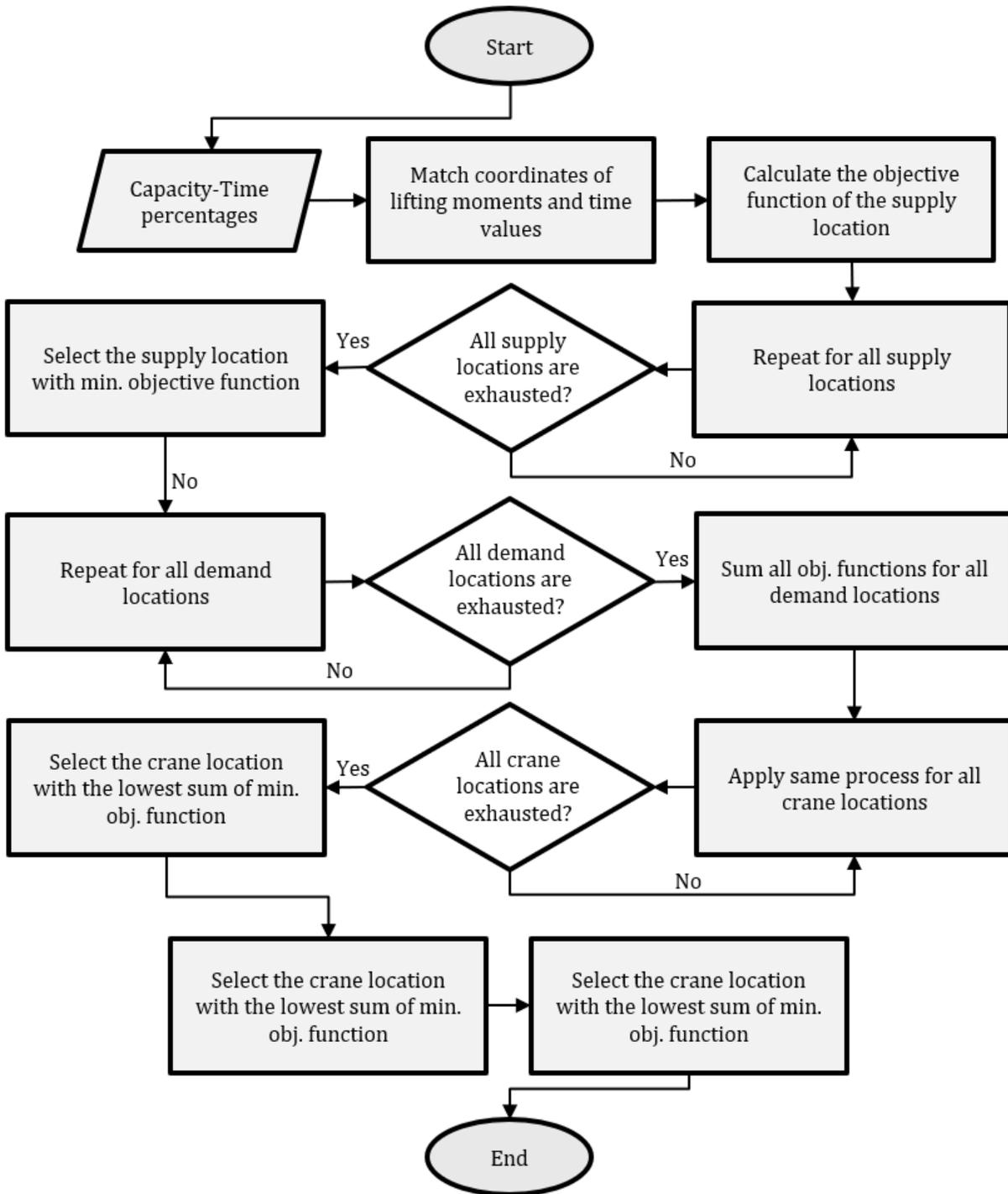
Fig 8. Flowchart of Twofold Distance-based-Mathematical Optimization

3.2 Extreme Wind Gusts Integration to Crane Model and Configuration Selection

Wind speeds are known to be unpredictable in magnitude and in duration. As a result, their impact on tower cranes can range from insignificant to very serious, in which case, structural failure can occur. To understand the impact of high-speed winds on crane stability and operation, mathematical and practical calculations must be judiciously performed to foresee the behavior of the lifting equipment. In spite of the uncertainty and approximation involved in the calculations, they are still mandatory. Anchoring or ballasting of the tower crane base could mitigate the risk overturning, even though, a tower crane's mast is a structural beam which deflects under the footprint of imbalanced loads and dynamic wind forces. Crane manufacturers thus follow established standards (e.g., ASCE in North America, and FEM elsewhere around the world) when designing structures that are competent to resist the effects of wind. In spite of these efforts, though, many crane accidents are still attributable to structural failure or overturning precipitated by wind pressure.

If a specific prospective crane location results in a lower magnitude of wind dynamic loads on the tower crane structure, this indicates that assigning this location for the erection and the remainder of the project's crane-related-processes is preferable [90]. This case is valid only if adjacent buildings to the tower crane exist, which mitigates detrimental effects of wind that lead to over-turning and torsion moments. In order to predict the effect of wind on tower crane operations, relevant data such as wind velocity and directionality are essential.

Anemometers are instruments that can determine velocity, magnitude, and direction of wind. However, anemometers are limited to daily operations and are in actuality inadequate for foreseeing future wind characteristics. As a result, approaches such as the Monte Carlo simulation and neural networks were, and still are, implemented for this purpose; such approaches depend

significantly on gathering historical wind data to predict future wind behavior [54,91,92]. However, collecting comprehensive and accurate historical wind data is a tedious endeavor. Moreover, the historical wind data must cover a sufficient time period. Therefore, a web scraping computer code using C# language and Selenium library was written specifically for the purpose of extracting hourly wind-pertinent information over a time period of five years. Ultimately, this leads to saving the data in the form of a CSV file for compatibility purposes. The static wind analysis examines the aloft tower crane's functionality under high wind speeds. Thus, the maximum wind velocity value will be extracted from the CSV file, although the data can be further employed for predicting hourly future velocities and directions in the context of scheduling tower crane operations and to determine the tower crane's workability status.

Normally, tower crane design considers both in-service and out-of-service wind conditions, since wind aerodynamics vary with each case. However, crane stability is usually dictated by the out-of-service condition [93].
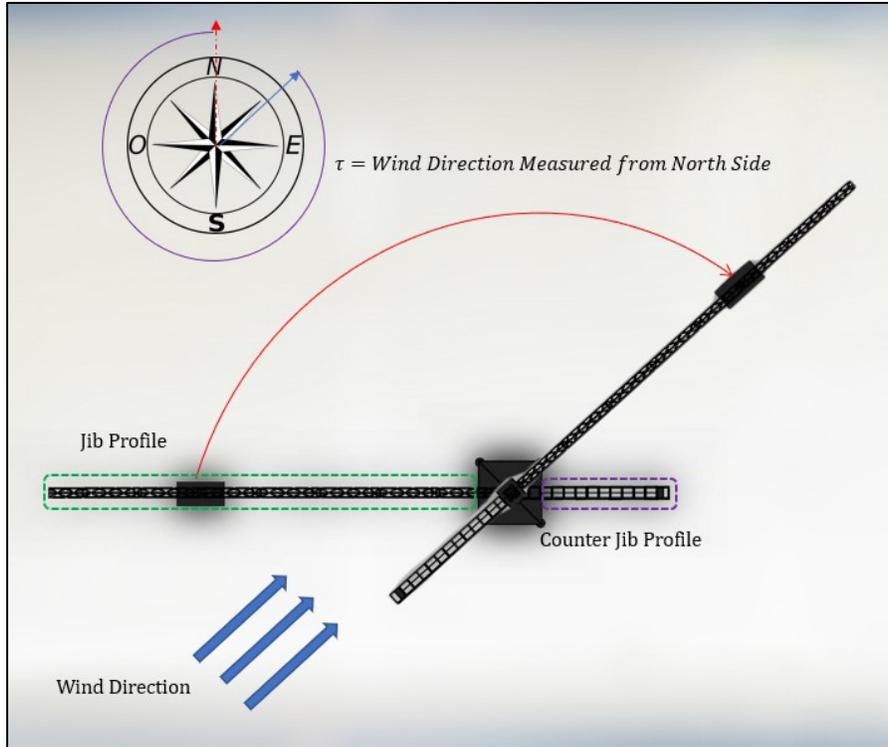
Fig 9. Effect of weathervane on tower crane jib

Wind, which is by nature random and unpredictable, exposes tower cranes to torsion and overturning moment, where rear-to-front wind F_{front} and the lifted load act as actuators for frontward moment and, front-to-rear F_{rear} wind and the counterweight load are the same with respect to rearward moment (see Fig 12). On the other hand, oscillation of the lifted load, slewing trajectory, and wind in the direction perpendicular to the jib induce torsion moments. It should be noted, torsion moments are not within our scope. By virtue of Equation (11), influencing wind pressure q is dependent proportionally on the total height h and the square of the velocity v, resulting in a dramatic increase in pressure as wind velocity increases.

$$q = \frac{5}{8}v^2 \qquad\qquad (11)$$

As such, tower cranes are not permitted to operate legitimately beyond wind speeds of 20 m/s. Additionally, the tower crane jib must be unlocked when in an idle state to allow the jib to swing freely which mitigate the bending moments on the tower crane base. This orientation of the jib minimizes its profile's exposure to the wind direction, since the jib's cross-section area is larger than that of the counter-jib's (see Fig 9). Neglecting the lifted module in Fig 12, we see that, in case of an idle tower crane, the counter jib's bending moment magnitude is predominant to the jib's. Accordingly, the supplemental stability of the tower crane structure is linked to the weathervane phenomena because of the added moment to the jib's moment, given that they are directionally identical.

Consequently, in the present study, for all the above-mentioned factors, the focus is on out-of-service conditions lifted rather than in-service conditions. Moreover, load dynamics and slewing accelerations will be overshadowed for more simplicity. In this regard, defining the magnitude of the base overturning to the front or rear, the over-the-side moments and the horizontal deformation distance from the vertical location of the top part of the mast, could provide planners with a better frame of reference.

The proposed static wind analysis is a provisional approach integrating the aforementioned aspects that increase the robustness of decision making with respect to selecting a suitable, reliable tower crane model, and configurations. First, the support reactions of the tower crane legs,

P_{fb}, P_{rb}, P_{fc}, P_{rc}, are calculated using an analytical method to dissect the corollary of wind velocity and direction for up to 360° rotation of the jib. (See Fig 10, which shows 3 negative reactions resulting in tower crane overturning). In this context, if the crane can be configured and operated in either a free standing (normally happens when the tower crane height is low, and no wind occurrence is expected) or a fixation to the ground mode is a required through anchoring or ballast-base attachments. Anchorage bolts design and selection is not within our scope therefore knowing all the forces will help in determining the crane ballast base configurations by the proposed methodology. Fig 11 depicts a rudimentary schematic of the integration of wind effects in the evaluation of tower crane models and configurations.
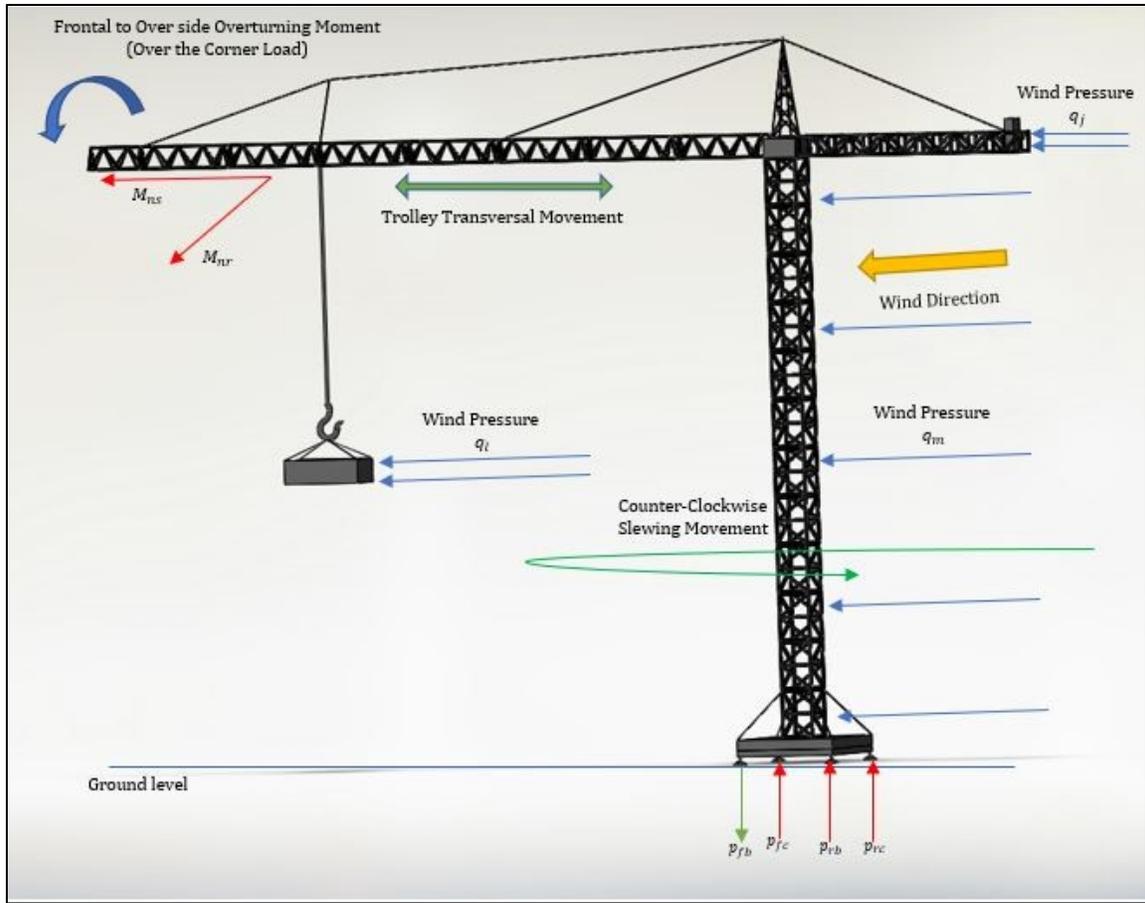
Fig 10. Wind induced frontward and over the side moment and their effect on tower crane legs ground bearing pressures
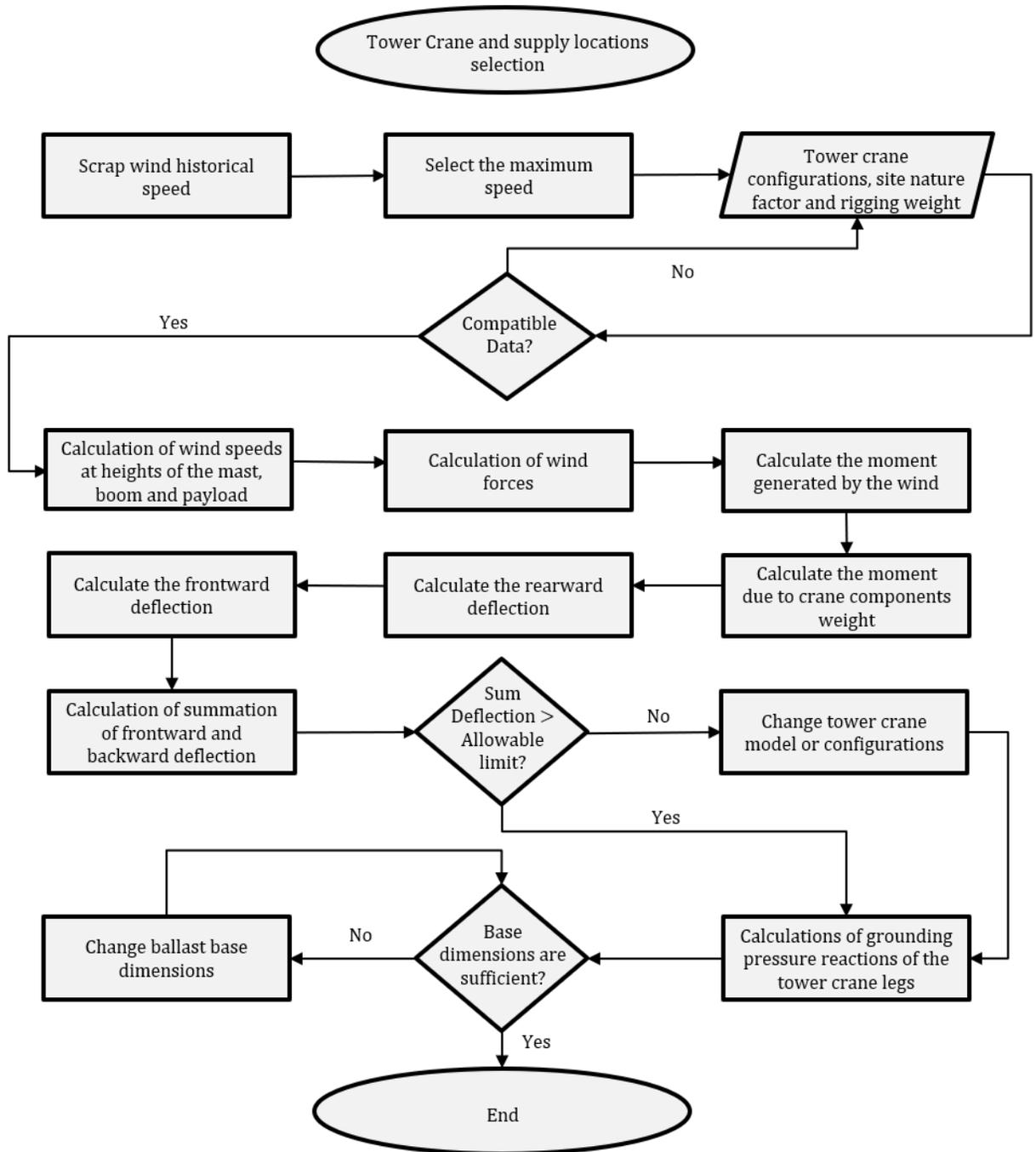
Fig 11. Flowchart for integrating extreme wind speeds into crane model and configuration selections

3.2.1 Calculation of Overturning Resistance and Tower Crane Ballast Base Dimensions

An important prerequisite for wind analysis is to extract all the tower crane components

specifications; (height, width, length, weight) from the manufacturer's data sheet. Globally, all tower crane models have masts with heights in excess of 10 m Hence, various mathematical formulas have developed to extrapolate wind speed data to different heights (e.g., Power Law, Extended Power Law, Weibull Distribution Parameter Extrapolation). Monin-Obukhov's similarity theory was the mainspring for the similarity Model known as Power Law [94] — the theory selected for the calculations in the present research. Equation (12) represents this theory where $v_\circ$ is wind speed monitored at $h_\circ$ height of 10 m and h is the tower crane's height. The power-law exponent δ value, it should be noted, depends on the construction location. In this regard, A.G Davenport [95] suggested the values of 1/9 for unobstructed areas and water surfaces, 1/7 for coastal areas and open country, 1/4 for urban and suburban areas and 1/3 for large cities centers.

$$v = v_\circ \left(\frac{h}{h_\circ}\right)^\delta \tag{12}$$

As Fig 12 shows, the wind pressure q will affect the structure of the latticed mast, jib and the lifted object throughout the lifting operation. A tower crane's cross-section is not a solid body; accordingly, Shapiro and Shapiro [93] listed different values of wind-pressure coefficient based on diverse crane designs, and defined the ratio between the sum of the face areas of members in the frame and gross area enclosed by the borders of the frame.

Therefore, a resultant force F on the tower crane components or the lifted module will be generated directly proportional to its rectangular cross-section area A, wind pressure q and C_f as shown in Equation (13).

$$F = qAC_f \qquad\qquad (13)$$

Accounting for the worst-case scenario, the largest area of the cross-section is used in the calculations (the cross-section changes relatively based on the angle of the wind direction). The resultant wind forces exerted on other components of the tower crane (e.g., tension rods, trolley, gantry, rigging system) are not continued because of the insignificant cross-section areas of those components.

The tower crane base bending moment represents the summation of each resultant force, multiplied by the vertical distance between where the wind force is applied on each component and the tower crane base. Owing to the regularity and uniformity of the mast, jib, and most of the lifted objects, it is assumed that the point where the wind force is applied on an object is the centroid.

Fig 12 delineates the procedure for calculating the wind forces in the cases of saddle and luffing tower crane, where q_m, q_j, q_l, F_m, F_j, F_l, H_m, H_j, H_l are the wind pressures, resultant forces, and the vertical distances between the ground level and the centroid for the mast, jib, and lifted object, respectively. As for the mast, the centroid is located at the midpoint of its height measured from the ground level to the top of the mast. In contrast, in the case of the jib, the height where the wind effect is applied, is assessed as the mast height plus half of the height of the jib's cross-section, where for the lifted object, the height will be 10 m (since wind speed is measured at 10 m above the ground) [87]. The bending moment over the tower crane base triggered by the wind forces can be estimated accordingly through Equation (20).

$$M_w = F_m . H_m + F_j . H_j + F_l . H_l \qquad (14)$$
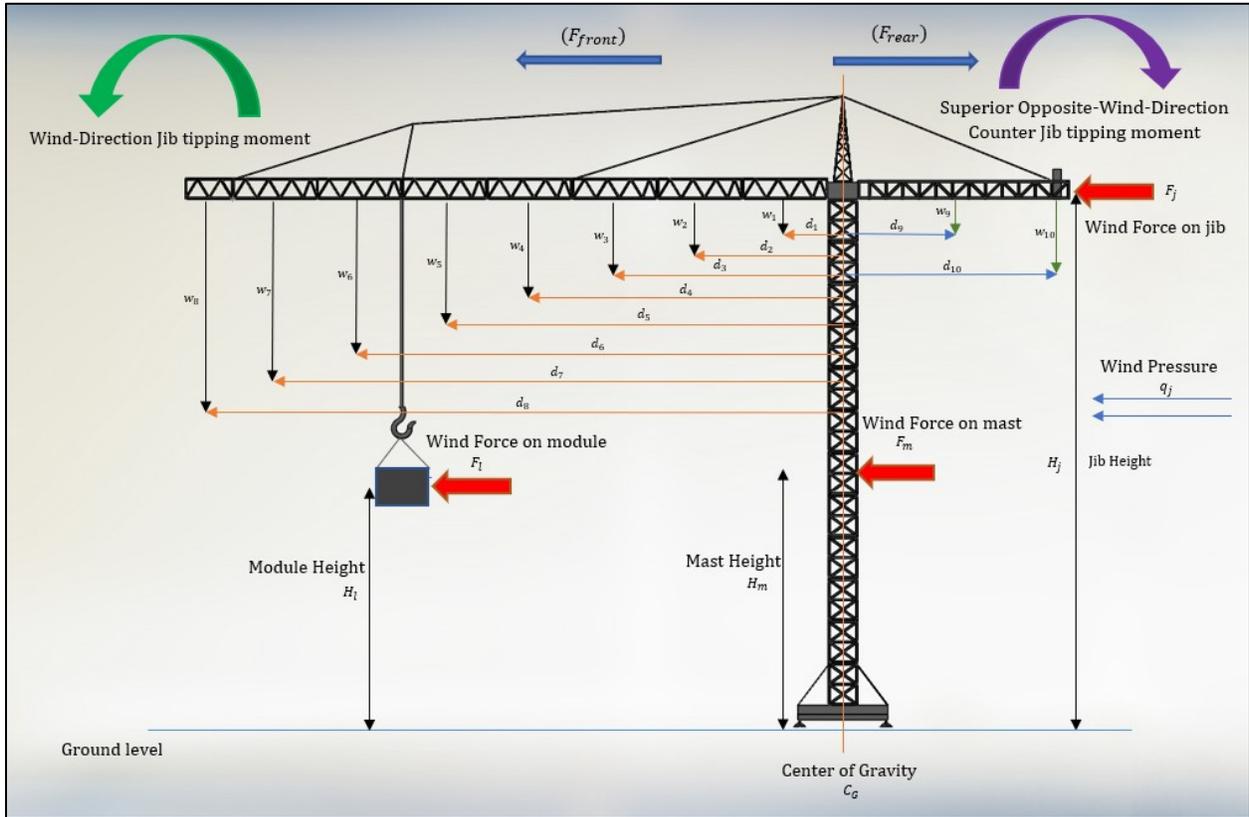
Fig 12. Presentation of wind effect and forces and procedure for calculating wind and ultimate moment

A free standing anchored or ballast-based tower crane, it should be noted, is still susceptible to bending moments around the CG of the crane (i.e., the centroid) even in the absence of wind-induced forces. In the case of the tower crane anchorage to the terrain, transfers all the vertical loads and shear forces from the mast to the ground due to the predominant weight of the ballast base. Practically, the ballast base surface and mast centroids must be located concentrically. Furthermore, since the mast's cross section is typically square or rectangular. tower crane fixation modes shift the CG of the overall system to be concentric with the projection of the CG of the

mast.

In this respect, tower crane components' CGs not coinciding with the axes of projection of the centroid will amplify the bending moment on the tower crane mast.. These components, it should be noted, consist primarily of the structural components of the jib, counter-jib and all associated accessories (e.g., trolley, counterweight) in addition to the lifted object. This is in contrast, to parts of the mast and the over tower structures which do not exert bending moment on the mast. Thus, and with working over the day cycle times, tower crane legs undergo tension and compression. Two categories of phenomena can be observed in response to the resultant bending moments.

The first acts around the crane sides and the other acts on the forefront or tail of the crane. Both categories are functions of the ultimate moment and the swinging angle of the tower crane jib. A top-slewing tower cranes jib and counter-jib components apply opposite directional bending moments respectively, thereby helping to stabilize and reducing the risk of overturning of the whole structure in both in-service and out of service condition, bearing in mind the influence of the generated moment of the critical weight. Equation (15) identifies the ultimate moment M_u, which is sum of the total bending moments for all components whose CG is not coterminous with that of the tower crane. w_{ji} and l_{ji} are, respectively, weight and length of ji as a member in the jib set JI. Similarly, with CJ as the counter jib set where w_{cj} and l_{cj} are respectively weight and length of cj as a member in the counter jib set J . It is important to mention that weights the jib and counter jib elements are discretized in the present study for more precise calculation due to their different weights (see Fig 12).

$$M_u = \sum_{ji}^{JI} w_{ji} \cdot l_{ji} - \sum_{cj}^{CJ} w_{cj} \cdot l_{cj} \qquad (15)$$

Subsequently, the moments around the crane sides M_{ns} and rear or front M_{nr} can be derived as Equations (16) and (17) show as function of the following factors:

- The ultimate moment M_u.

- The wind moment M_w.

- The horizontal swinging angle of the tower crane ω (see Fig 5).

- The wind direction measured from the north counterclockwise τ (see Fig 9).

- The sum of all vertical loads V_u.

- The distance between the tower crane's center of gravity and center of rotation $x_\circ$.

A tower crane's center of gravity and rotation are concentric. This is due to the shifting of the tower crane's CG which is impacted by anchorage, as previously mentioned. Therefore, $x_\circ$ value is always considered zero.

$$M_{ns} = M_u \sin\alpha - M_w \sin(\tau - \omega) \qquad (16)$$

$$M_{nr} = M_u \cos\alpha - M_w \cos(\tau - \omega) - V_u x_\circ \qquad (17)$$

The tower crane legs' reactions are a function of their mass of the tower crane and their

values change simultaneously with the tower crane's slewing and transversal movements. For instance, while maneuvering a heavy load with the jib axis coinciding with the axis of the centroids of two legs concurrently, the load being lifted over the corner of the tower crane exerts the lowest pressure on the furthest leg away from the lifted load. On the contrary, the highest reaction is applied with the other as they are unproportionally interrelated as shown in Fig 10 where P_{fb} represents furthest corner from the lifted load and minimum reaction. Increasing or decreasing the lifting radius amplifies or depletes the first, unlike the second, respectively. This case occurs when the horizontal slewing angle is at a 45°, 135°, 225°, or 315° angle relative to the y-axis parallel to the width and normal to the length of the base. A negative pressure, it should be noted, exhibits itself in the form of a leg losing contact with the ground, as Fig 10 illustrates, a situation which, exhibits itself in the form of a leg losing contact with the ground. Equations (18) - (21) demonstrate that Reactions on four legs are functions of front-rear and over the side moments, vertical weight, and longitudinal d_l and transverse distances d_t of tower crane legs (see Fig 14). Given that the design of crane components is outside the scope of the present study, the total vertical load is the only adjustable parameter to be considered in amending the ballast base dimensions or the type of the anchor bolts.

$$P_{fb} = \frac{V_u}{4} + \frac{1}{2}\left(\frac{M_{ns}}{d_t} - \frac{M_{nr}}{d_l}\right) \tag{18}$$

$$P_{rb} = \frac{V_u}{4} + \frac{1}{2}\left(\frac{M_{ns}}{d_t} + \frac{M_{nr}}{d_l}\right) \tag{19}$$

$$P_{fc} = \frac{V_u}{4} - \frac{1}{2}\left(\frac{M_{ns}}{d_t} + \frac{M_{nr}}{d_l}\right) \tag{20}$$

$$P_{rc} = \frac{V_u}{4} - \frac{1}{2}\left(\frac{M_{ns}}{d_t} - \frac{M_{nr}}{d_l}\right) \tag{21}$$

3.2.2 Feasibility of the Tower Crane Model and Mast Deflection Calculation

A tower crane mast is an elastic structural member. During out-of-service tower states, the mast deflects backwards, and plumbness is achieved as a result of the greater rearward counterweight moment. As mentioned earlier, in the presence of high wind velocities, the wind moment will be directionally opposite to the counterweight moment, owing to the weathervane effect. This elastic deformation exerts shear stresses on the small mast structural member's cross-sections and deviates the top members of the mast from the designed vertical course.

$$\delta = \delta_w + \delta_c \tag{22}$$

The total deflection δ is the sum of the deflections induced by the counterweight δ_c, and the high wind velocities δ_w as Equation (22) explains. The total deflection is the horizontal deflection of the y-axis of the mast measured from where the top part of the mast starts (one-third of the mast length) to the tip of the mast as Fig 13 demonstrates.

$$\delta_c = \frac{M_u}{Q}\left(\frac{1 - \cos kh}{\cos kh}\right) \tag{23}$$

Equation (23) explains the calculation of the mast backward deformation triggered because of the counterweight δ_c, where M_u is the ultimate moment generated due to the tower crane elements weights and distances from the tower crane CG. Noteworthy, the sum of the top one-third of the mast weight and the slewing component weight of the tower crane is referred as Q and h is the height of the tower crane mast. As per Equation (24)

$$k = \left(\frac{Q}{EI}\right)^{\frac{1}{2}} \tag{24}$$

k is a function of Young Modulus E; the stiffness or the material capability of deformation and the second moment of area I, which, in turn, correlates with the mast cross face and the area enclosed by the mast frame borders (as shown in Fig 14). I is estimated through Equation (25)

$$I = (Mf_w)^2 * Mast_w * Mast_l \tag{25}$$

Where Mf_w is the width of cross section of the tower crane section (a tower crane mast consists of multiple tower crane sections), $Mast_w$ is the width of the mast structure and $Mast_l$ is the length

of the mast structure as shown in Fig 14. Afterwards, the deflection induced by wind moments δ_w

of can be obtained through Equation (26)

$$\delta_w = \frac{1}{Qk}\left[w_w(\tan kh - kh) + \sigma h\left(\tan kh - \frac{kh}{2}\right) - \frac{\sigma}{k}\frac{1 - \cos kh}{\cos kh}\right] \tag{26}$$

Where σ is wind force per unit of length on the mast and w_w is the wind force on the center of the

cross section of the area above the slewing ring. Fig 13 demonstrates the mast's horizontal

deformation. Crane manufacturers, it should be noted, have different design tolerances regarding

the divergence of the mast, nonetheless, all cranes are subject to plumbness tolerance of 1:500 for

adequate safety requirements, and up to 1:1000 for rigorous protection procedures [47]. The total

deflection is compared to the abovementioned consensuses tolerances of the tower crane mast

deflection and if the total deflection is not within the limits; the tower crane configurations or

model must be altered.
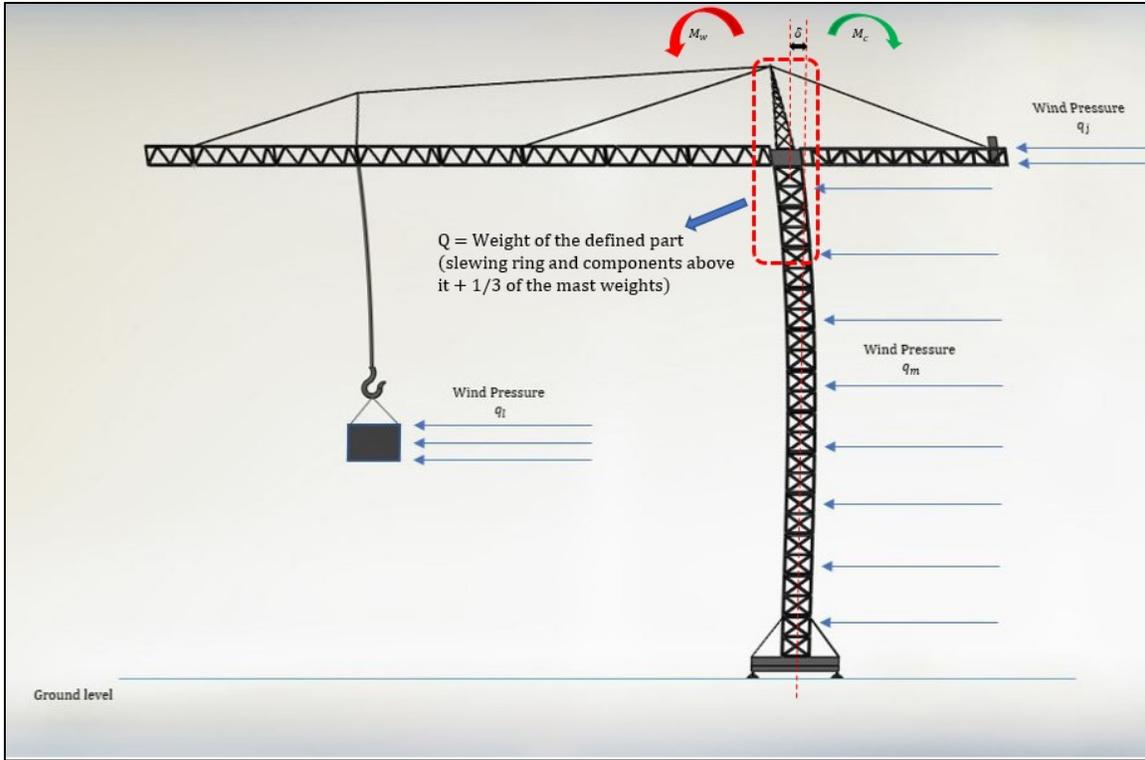
Fig 13. Wind induced frontward and over the side moment and their effect on tower crane legs ground bearing pressures
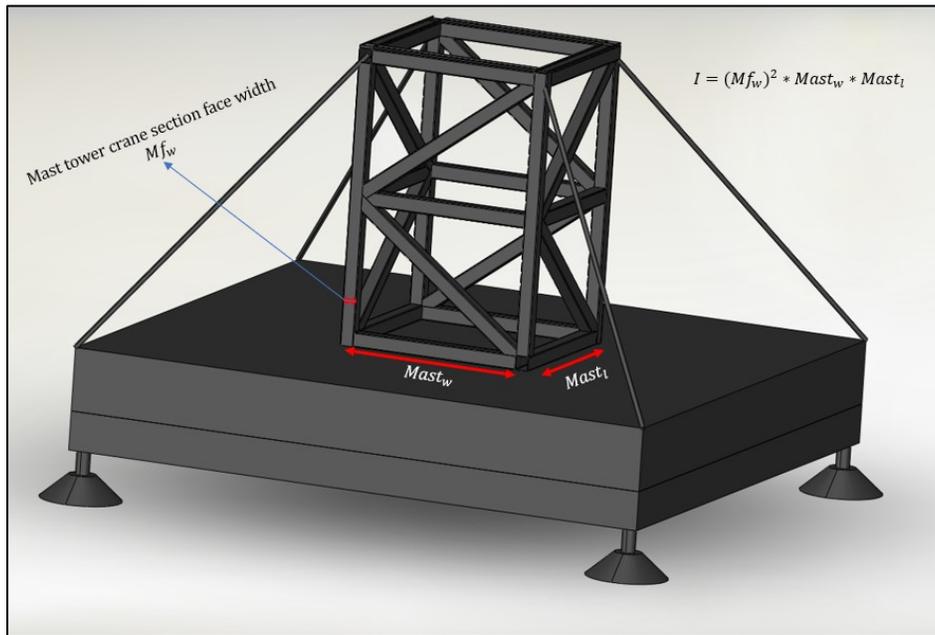
Fig 14. Mast physical properties affecting the second moment of inertia

Chapter 4: Case Studies

4.1 Hypothetical Case Study

To determine the feasibility of the methodology, a case study of a 34-storey building, consist of 950 structural steel modules, and located in New York City, was considered. The site layout configurations (e.g., tower crane location, material supply locations) were designated in such as manner as to minimize the optimization variable, $O_{k,s,d,c}$. The developed computer program was frontloaded with 514 potential tower crane location coordinates, and the same coordinates were adopted also for potential material supply locations. Each storey contained 32 demand locations at which to place the modules. Coordinate information and module dimensions and weights were rendered in a Microsoft Excel file.
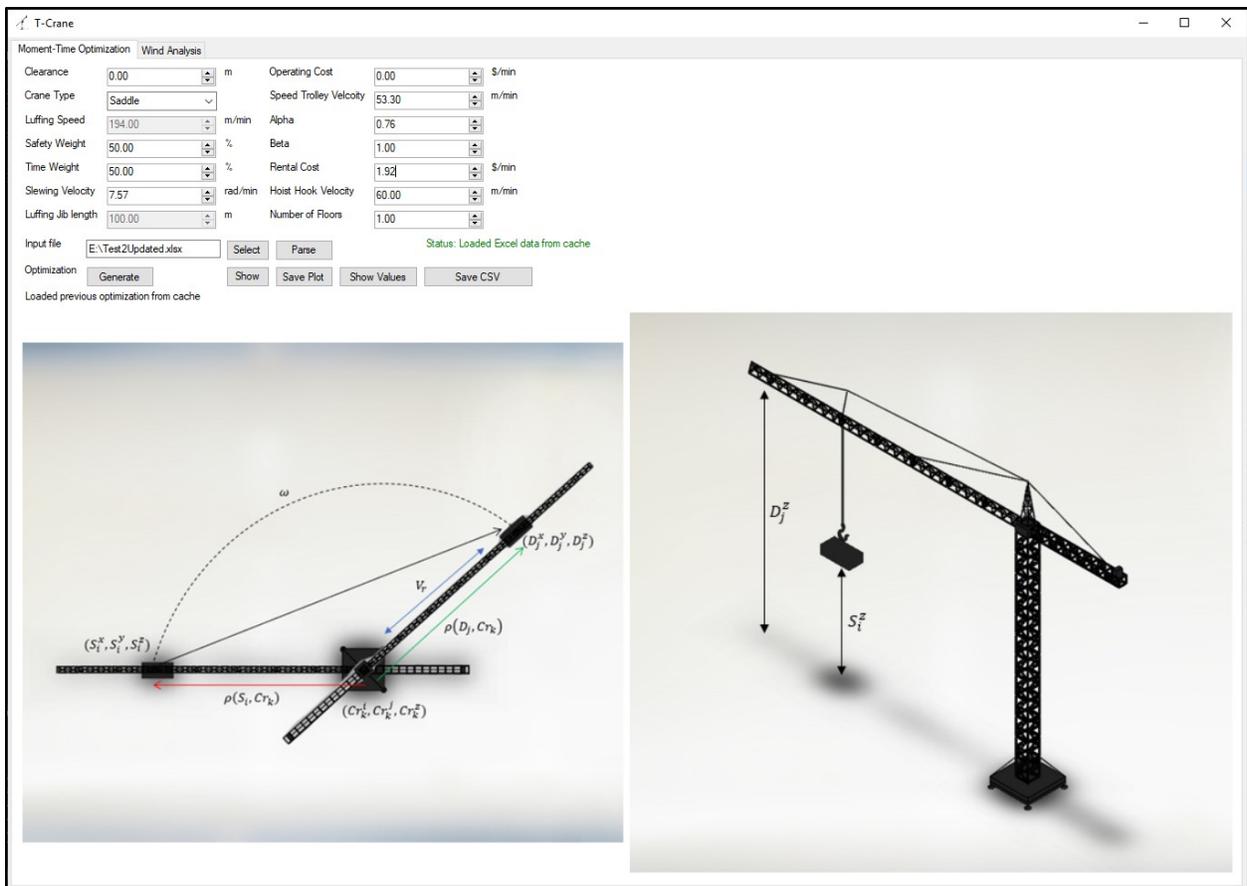
Fig 15. Graphical User Interface of site Layout Optimization tab

Fig 15, shows the graphical user interface (GUI) within the site layout optimization tab. The GUI embodies boxes for the decision makers to input various variables of tower crane specifications. AS can be seen, it features boxes in which for the user to input:

- The tower crane type selecting between a saddle or luffing tower crane.

- Clearance.

- Percentile weight of the operation time and safety.

- Velocities of the tower crane.

- Configurations of Zhang [65] operation time formulas and rental and operating cost.

- The file directory of the excel file which contains information of the site coordinates and modules as shown in Table 2.

The following assumptions were adopted; crane velocities, V_r, V_ω, V_h of 53.3 m/min, 7.57 rad/min and 60 m/min, respectively, 1 m clearance, operating cost of 1.92 \$/min, rental cost of 0 \$/min (due to a lack of tower crane rental prices). The input parameters for the second part of the algorithm, derived from Zhang et al. [65], were set as α = 0.25, β = 1.0 which are considered variables of the crane operator mastery. All crane locations have the degree of operating complexity therefore γ_k= 1.0.

The generated form includes information about the selected crane location, a list of the material supply locations each assigned to a demand location, the maximum radius the tower crane can accommodate, the total operating time (excluding hooking, unhooking, and weight alignment), and the total cost. Table 3 summarizes the results of discrete capacity/time weights.

As can be seen in the table, the algorithm tends toward generating crane locations and supply locations at greater distances from one another and from the demand locations as more weight is shifted to operation time.

Moreover, total cost was found in this study to be inversely correlated with operation time, meaning that a lower operation time results in a lower cost. Although this is not realistic because the rental cost of the tower crane is not included in calculations, nevertheless the option of choosing higher operation time weight (lower operation time) is beneficial to decision makers if there is tendency to faster crane operations because of tight schedules. Omitting the capacity weight, it should be noted, intensifies the maximum moment exposed, thereby increasing the total cost significantly (This phenomenon is explained further in reference to the Nadoushani case study in the following section). On the other hand, a higher weight being assigned to capacity directs the algorithm to decrease lifting radiuses. Fig 16 shows an automatically generated plot of all site coordinates defining precisely all selected crane and material supply locations.
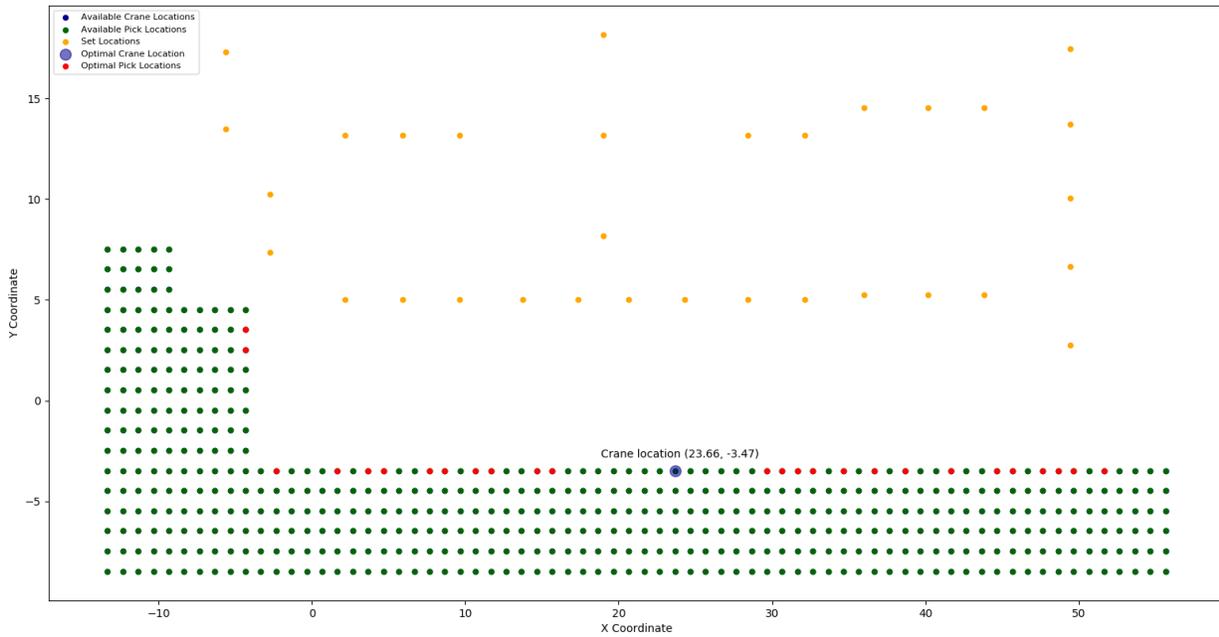
Fig 16. Automatic plot to case study 1 site coordinates representing crane, supply and demand locations

Table 2 Site Layout Coordinates and Module Information

No.	Crane locations			Supply locations			Demand locations			Module information			
	Cr_k^x	Cr_k^y	Cr_k^z	S_i^X	S_i^y	S_i^z	D_j^x	D_j^y	D_j^z	W_j	length	width	height
1.	-13.34	7.53	0	-13.34	7.53	0	-5.64	17.3	0	13.6	11.45	3.76	3
2.	-12.34	7.53	0	-12.34	7.53	0	-5.64	13.49	0	17.48	11.45	3.96	3
3.	-11.34	7.53	0	-11.34	7.53	0	-2.74	10.24	0	5.27	5.75	2.74	3
4.	-10.34	7.53	0	-10.34	7.53	0	-2.74	7.34	0	6.49	5.75	3.18	3
5.	-9.34	7.53	0	-9.34	7.53	0	2.13	5.03	0	15.65	4.32	10.36	3
6.	-13.34	6.53	0	-13.34	6.53	0	5.89	5.03	0	11.79	3.25	10.36	3

7.	-12.34	6.53	0	-12.34	6.53	0	9.6	5.03	0	15.1	4.17	10.36	3
8.	-11.34	6.53	0	-11.34	6.53	0	13.72	5.03	0	14.73	4.06	10.36	3
9.	-10.34	6.53	0	-10.34	6.53	0	17.37	5.03	0	11.79	3.25	10.36	3
10.	-9.34	6.53	0	-9.34	6.53	0	20.62	5.03	0	11.79	3.25	10.36	3
11.	-13.34	5.53	0	-13.34	5.53	0	24.28	5.03	0	14.73	4.06	10.36	3
12.	-12.34	5.53	0	-12.34	5.53	0	28.4	5.03	0	15.1	4.17	10.36	3
13.	-11.34	5.53	0	-11.34	5.53	0	32.11	5.03	0	11.79	3.25	10.36	3
14.	-10.34	5.53	0	-10.34	5.53	0	35.99	5.26	0	14.27	4.32	9.35	3
15.	-9.34	5.53	0	-9.34	5.53	0	40.18	5.26	0	13.43	4.06	9.35	3
16.	-13.34	4.53	0	-13.34	4.53	0	43.84	5.26	0	10.75	3.25	9.35	3
17.	-12.34	4.53	0	-12.34	4.53	0	49.45	2.74	0	11.91	7.98	4.27	3
18.	-11.34	4.53	0	-11.34	4.53	0	49.45	6.65	0	9.92	7.98	3.56	3
19.	-10.34	4.53	0	-10.34	4.53	0	49.45	10.06	0	9.07	7.98	3.25	3
20.	-9.34	4.53	0	-9.34	4.53	0	49.45	13.72	0	11.34	7.98	4.06	3
21.	-8.34	4.53	0	-8.34	4.53	0	49.45	17.48	0	9.64	7.98	3.45	3
22.	-7.34	4.53	0	-7.34	4.53	0	43.84	14.55	0	10.4	3.25	9.04	3
23.	-6.34	4.53	0	-6.34	4.53	0	40.18	14.55	0	13	4.06	9.04	3
24.	-5.34	4.53	0	-5.34	4.53	0	35.99	14.55	0	15.19	4.32	9.96	3
25.	-4.34	4.53	0	-4.34	4.53	0	32.11	13.16	0	11.44	3.25	9.96	3
26.	-13.34	3.53	0	-13.34	3.53	0	28.4	13.16	0	14.66	4.17	9.96	3
27.	-12.34	3.53	0	-12.34	3.53	0	19	18.16	0	17.55	14.63	3.4	3
28.	-11.34	3.53	0	-11.34	3.53	0	19	13.16	0	9.36	14.63	3.28	3
29.	-10.34	3.53	0	-10.34	3.53	0	19	8.16	0	9.36	14.63	3.28	3

#													
30.	-9.34	3.53	0	-9.34	3.53	0	9.6	13.16	0	14.66	4.17	9.96	3
31.	-8.34	3.53	0	-8.34	3.53	0	5.89	13.16	0	11.44	3.25	9.96	3
32.	-7.34	3.53	0	-7.34	3.53	0	2.13	13.16	0	15.19	4.32	9.96	3
33.	-6.34	3.53	0	-6.34	3.53	0							
34.	-5.34	3.53	0	-5.34	3.53	0							
35.	-4.34	3.53	0	-4.34	3.53	0							
36.	-13.34	2.53	0	-13.34	2.53	0							
37.	-12.34	2.53	0	-12.34	2.53	0							
38.	-11.34	2.53	0	-11.34	2.53	0							
39.	-10.34	2.53	0	-10.34	2.53	0							
40.	-9.34	2.53	0	-9.34	2.53	0							
41.	-8.34	2.53	0	-8.34	2.53	0							
42.	-7.34	2.53	0	-7.34	2.53	0							
43.	-6.34	2.53	0	-6.34	2.53	0							
44.	-5.34	2.53	0	-5.34	2.53	0							
45.	-4.34	2.53	0	-4.34	2.53	0							
46.	-13.34	1.53	0	-13.34	1.53	0							
47.	-12.34	1.53	0	-12.34	1.53	0							
48.	-11.34	1.53	0	-11.34	1.53	0							
49.	-10.34	1.53	0	-10.34	1.53	0							
50.	-9.34	1.53	0	-9.34	1.53	0							
51.	-8.34	1.53	0	-8.34	1.53	0							
52.	-7.34	1.53	0	-7.34	1.53	0							

53.	-6.34	1.53	0	-6.34	1.53	0								
54.	-5.34	1.53	0	-5.34	1.53	0								
55.	-4.34	1.53	0	-4.34	1.53	0								
56.	-13.34	0.53	0	-13.34	0.53	0								
57.	-12.34	0.53	0	-12.34	0.53	0								
58.	-11.34	0.53	0	-11.34	0.53	0								
59.	-10.34	0.53	0	-10.34	0.53	0								
60.	-9.34	0.53	0	-9.34	0.53	0								
61.	-8.34	0.53	0	-8.34	0.53	0								
62.	-7.34	0.53	0	-7.34	0.53	0								
63.	-6.34	0.53	0	-6.34	0.53	0								
64.	-5.34	0.53	0	-5.34	0.53	0								
65.	-4.34	0.53	0	-4.34	0.53	0								
66.	-13.34	-0.47	0	-13.34	-0.47	0								
67.	-12.34	-0.47	0	-12.34	-0.47	0								
68.	-11.34	-0.47	0	-11.34	-0.47	0								
69.	-10.34	-0.47	0	-10.34	-0.47	0								
70.	-9.34	-0.47	0	-9.34	-0.47	0								
71.	-8.34	-0.47	0	-8.34	-0.47	0								
72.	-7.34	-0.47	0	-7.34	-0.47	0								
73.	-6.34	-0.47	0	-6.34	-0.47	0								
74.	-5.34	-0.47	0	-5.34	-0.47	0								
75.	-4.34	-0.47	0	-4.34	-0.47	0								

76.	-13.34	-1.47	0	-13.34	-1.47	0							
77.	-12.34	-1.47	0	-12.34	-1.47	0							
78.	-11.34	-1.47	0	-11.34	-1.47	0							
79.	-10.34	-1.47	0	-10.34	-1.47	0							
80.	-9.34	-1.47	0	-9.34	-1.47	0							
81.	-8.34	-1.47	0	-8.34	-1.47	0							
82.	-7.34	-1.47	0	-7.34	-1.47	0							
83.	-6.34	-1.47	0	-6.34	-1.47	0							
84.	-5.34	-1.47	0	-5.34	-1.47	0							
85.	-4.34	-1.47	0	-4.34	-1.47	0							
86.	-13.34	-2.47	0	-13.34	-2.47	0							
87.	-12.34	-2.47	0	-12.34	-2.47	0							
88.	-11.34	-2.47	0	-11.34	-2.47	0							
89.	-10.34	-2.47	0	-10.34	-2.47	0							
90.	-9.34	-2.47	0	-9.34	-2.47	0							
91.	-8.34	-2.47	0	-8.34	-2.47	0							
92.	-7.34	-2.47	0	-7.34	-2.47	0							
93.	-6.34	-2.47	0	-6.34	-2.47	0							
94.	-5.34	-2.47	0	-5.34	-2.47	0							
95.	-4.34	-2.47	0	-4.34	-2.47	0							
96.	-13.34	-3.47	0	-13.34	-3.47	0							
97.	-12.34	-3.47	0	-12.34	-3.47	0							
98.	-11.34	-3.47	0	-11.34	-3.47	0							

99.	-10.34	-3.47	0	-10.34	-3.47	0							
100.	-9.34	-3.47	0	-9.34	-3.47	0							
101.	-8.34	-3.47	0	-8.34	-3.47	0							
102.	-7.34	-3.47	0	-7.34	-3.47	0							
103.	-6.34	-3.47	0	-6.34	-3.47	0							
104.	-5.34	-3.47	0	-5.34	-3.47	0							
105.	-4.34	-3.47	0	-4.34	-3.47	0							
106.	-3.34	-3.47	0	-3.34	-3.47	0							
107.	-2.34	-3.47	0	-2.34	-3.47	0							
108.	-1.34	-3.47	0	-1.34	-3.47	0							
109.	-0.34	-3.47	0	-0.34	-3.47	0							
110.	0.66	-3.47	0	0.66	-3.47	0							
111.	1.66	-3.47	0	1.66	-3.47	0							
112.	2.66	-3.47	0	2.66	-3.47	0							
113.	3.66	-3.47	0	3.66	-3.47	0							
114.	4.66	-3.47	0	4.66	-3.47	0							
115.	5.66	-3.47	0	5.66	-3.47	0							
116.	6.66	-3.47	0	6.66	-3.47	0							
117.	7.66	-3.47	0	7.66	-3.47	0							
118.	8.66	-3.47	0	8.66	-3.47	0							
119.	9.66	-3.47	0	9.66	-3.47	0							
120.	10.66	-3.47	0	10.66	-3.47	0							
121.	11.66	-3.47	0	11.66	-3.47	0							

122.	12.66	-3.47	0	12.66	-3.47	0								
123.	13.66	-3.47	0	13.66	-3.47	0								
124.	14.66	-3.47	0	14.66	-3.47	0								
125.	15.66	-3.47	0	15.66	-3.47	0								
126.	16.66	-3.47	0	16.66	-3.47	0								
127.	17.66	-3.47	0	17.66	-3.47	0								
128.	18.66	-3.47	0	18.66	-3.47	0								
129.	19.66	-3.47	0	19.66	-3.47	0								
130.	20.66	-3.47	0	20.66	-3.47	0								
131.	21.66	-3.47	0	21.66	-3.47	0								
132.	22.66	-3.47	0	22.66	-3.47	0								
133.	23.66	-3.47	0	23.66	-3.47	0								
134.	24.66	-3.47	0	24.66	-3.47	0								
135.	25.66	-3.47	0	25.66	-3.47	0								
136.	26.66	-3.47	0	26.66	-3.47	0								
137.	27.66	-3.47	0	27.66	-3.47	0								
138.	28.66	-3.47	0	28.66	-3.47	0								
139.	29.66	-3.47	0	29.66	-3.47	0								
140.	30.66	-3.47	0	30.66	-3.47	0								
141.	31.66	-3.47	0	31.66	-3.47	0								
142.	32.66	-3.47	0	32.66	-3.47	0								
143.	33.66	-3.47	0	33.66	-3.47	0								
144.	34.66	-3.47	0	34.66	-3.47	0								

145.	35.66	-3.47	0	35.66	-3.47	0								
146.	36.66	-3.47	0	36.66	-3.47	0								
147.	37.66	-3.47	0	37.66	-3.47	0								
148.	38.66	-3.47	0	38.66	-3.47	0								
149.	39.66	-3.47	0	39.66	-3.47	0								
150.	40.66	-3.47	0	40.66	-3.47	0								
151.	41.66	-3.47	0	41.66	-3.47	0								
152.	42.66	-3.47	0	42.66	-3.47	0								
153.	43.66	-3.47	0	43.66	-3.47	0								
154.	44.66	-3.47	0	44.66	-3.47	0								
155.	45.66	-3.47	0	45.66	-3.47	0								
156.	46.66	-3.47	0	46.66	-3.47	0								
157.	47.66	-3.47	0	47.66	-3.47	0								
158.	48.66	-3.47	0	48.66	-3.47	0								
159.	49.66	-3.47	0	49.66	-3.47	0								
160.	50.66	-3.47	0	50.66	-3.47	0								
161.	51.66	-3.47	0	51.66	-3.47	0								
162.	52.66	-3.47	0	52.66	-3.47	0								
163.	53.66	-3.47	0	53.66	-3.47	0								
164.	54.66	-3.47	0	54.66	-3.47	0								
165.	55.66	-3.47	0	55.66	-3.47	0								
166.	-13.34	-4.47	0	-13.34	-4.47	0								
167.	-12.34	-4.47	0	-12.34	-4.47	0								

168.	-11.34	-4.47	0	-11.34	-4.47	0								
169.	-10.34	-4.47	0	-10.34	-4.47	0								
170.	-9.34	-4.47	0	-9.34	-4.47	0								
171.	-8.34	-4.47	0	-8.34	-4.47	0								
172.	-7.34	-4.47	0	-7.34	-4.47	0								
173.	-6.34	-4.47	0	-6.34	-4.47	0								
174.	-5.34	-4.47	0	-5.34	-4.47	0								
175.	-4.34	-4.47	0	-4.34	-4.47	0								
176.	-3.34	-4.47	0	-3.34	-4.47	0								
177.	-2.34	-4.47	0	-2.34	-4.47	0								
178.	-1.34	-4.47	0	-1.34	-4.47	0								
179.	-0.34	-4.47	0	-0.34	-4.47	0								
180.	0.66	-4.47	0	0.66	-4.47	0								
181.	1.66	-4.47	0	1.66	-4.47	0								
182.	2.66	-4.47	0	2.66	-4.47	0								
183.	3.66	-4.47	0	3.66	-4.47	0								
184.	4.66	-4.47	0	4.66	-4.47	0								
185.	5.66	-4.47	0	5.66	-4.47	0								
186.	6.66	-4.47	0	6.66	-4.47	0								
187.	7.66	-4.47	0	7.66	-4.47	0								
188.	8.66	-4.47	0	8.66	-4.47	0								
189.	9.66	-4.47	0	9.66	-4.47	0								
190.	10.66	-4.47	0	10.66	-4.47	0								

191.	11.66	-4.47	0	11.66	-4.47	0								
192.	12.66	-4.47	0	12.66	-4.47	0								
193.	13.66	-4.47	0	13.66	-4.47	0								
194.	14.66	-4.47	0	14.66	-4.47	0								
195.	15.66	-4.47	0	15.66	-4.47	0								
196.	16.66	-4.47	0	16.66	-4.47	0								
197.	17.66	-4.47	0	17.66	-4.47	0								
198.	18.66	-4.47	0	18.66	-4.47	0								
199.	19.66	-4.47	0	19.66	-4.47	0								
200.	20.66	-4.47	0	20.66	-4.47	0								
201.	21.66	-4.47	0	21.66	-4.47	0								
202.	22.66	-4.47	0	22.66	-4.47	0								
203.	23.66	-4.47	0	23.66	-4.47	0								
204.	24.66	-4.47	0	24.66	-4.47	0								
205.	25.66	-4.47	0	25.66	-4.47	0								
206.	26.66	-4.47	0	26.66	-4.47	0								
207.	27.66	-4.47	0	27.66	-4.47	0								
208.	28.66	-4.47	0	28.66	-4.47	0								
209.	29.66	-4.47	0	29.66	-4.47	0								
210.	30.66	-4.47	0	30.66	-4.47	0								
211.	31.66	-4.47	0	31.66	-4.47	0								
212.	32.66	-4.47	0	32.66	-4.47	0								
213.	33.66	-4.47	0	33.66	-4.47	0								

214.	34.66	-4.47	0	34.66	-4.47	0								
215.	35.66	-4.47	0	35.66	-4.47	0								
216.	36.66	-4.47	0	36.66	-4.47	0								
217.	37.66	-4.47	0	37.66	-4.47	0								
218.	38.66	-4.47	0	38.66	-4.47	0								
219.	39.66	-4.47	0	39.66	-4.47	0								
220.	40.66	-4.47	0	40.66	-4.47	0								
221.	41.66	-4.47	0	41.66	-4.47	0								
222.	42.66	-4.47	0	42.66	-4.47	0								
223.	43.66	-4.47	0	43.66	-4.47	0								
224.	44.66	-4.47	0	44.66	-4.47	0								
225.	45.66	-4.47	0	45.66	-4.47	0								
226.	46.66	-4.47	0	46.66	-4.47	0								
227.	47.66	-4.47	0	47.66	-4.47	0								
228.	48.66	-4.47	0	48.66	-4.47	0								
229.	49.66	-4.47	0	49.66	-4.47	0								
230.	50.66	-4.47	0	50.66	-4.47	0								
231.	51.66	-4.47	0	51.66	-4.47	0								
232.	52.66	-4.47	0	52.66	-4.47	0								
233.	53.66	-4.47	0	53.66	-4.47	0								
234.	54.66	-4.47	0	54.66	-4.47	0								
235.	55.66	-4.47	0	55.66	-4.47	0								
236.	-13.34	-5.47	0	-13.34	-5.47	0								

237.	-12.34	-5.47	0	-12.34	-5.47	0								
238.	-11.34	-5.47	0	-11.34	-5.47	0								
239.	-10.34	-5.47	0	-10.34	-5.47	0								
240.	-9.34	-5.47	0	-9.34	-5.47	0								
241.	-8.34	-5.47	0	-8.34	-5.47	0								
242.	-7.34	-5.47	0	-7.34	-5.47	0								
243.	-6.34	-5.47	0	-6.34	-5.47	0								
244.	-5.34	-5.47	0	-5.34	-5.47	0								
245.	-4.34	-5.47	0	-4.34	-5.47	0								
246.	-3.34	-5.47	0	-3.34	-5.47	0								
247.	-2.34	-5.47	0	-2.34	-5.47	0								
248.	-1.34	-5.47	0	-1.34	-5.47	0								
249.	-0.34	-5.47	0	-0.34	-5.47	0								
250.	0.66	-5.47	0	0.66	-5.47	0								
251.	1.66	-5.47	0	1.66	-5.47	0								
252.	2.66	-5.47	0	2.66	-5.47	0								
253.	3.66	-5.47	0	3.66	-5.47	0								
254.	4.66	-5.47	0	4.66	-5.47	0								
255.	5.66	-5.47	0	5.66	-5.47	0								
256.	6.66	-5.47	0	6.66	-5.47	0								
257.	7.66	-5.47	0	7.66	-5.47	0								
258.	8.66	-5.47	0	8.66	-5.47	0								
259.	9.66	-5.47	0	9.66	-5.47	0								

260.	10.66	-5.47	0	10.66	-5.47	0								
261.	11.66	-5.47	0	11.66	-5.47	0								
262.	12.66	-5.47	0	12.66	-5.47	0								
263.	13.66	-5.47	0	13.66	-5.47	0								
264.	14.66	-5.47	0	14.66	-5.47	0								
265.	15.66	-5.47	0	15.66	-5.47	0								
266.	16.66	-5.47	0	16.66	-5.47	0								
267.	17.66	-5.47	0	17.66	-5.47	0								
268.	18.66	-5.47	0	18.66	-5.47	0								
269.	19.66	-5.47	0	19.66	-5.47	0								
270.	20.66	-5.47	0	20.66	-5.47	0								
271.	21.66	-5.47	0	21.66	-5.47	0								
272.	22.66	-5.47	0	22.66	-5.47	0								
273.	23.66	-5.47	0	23.66	-5.47	0								
274.	24.66	-5.47	0	24.66	-5.47	0								
275.	25.66	-5.47	0	25.66	-5.47	0								
276.	26.66	-5.47	0	26.66	-5.47	0								
277.	27.66	-5.47	0	27.66	-5.47	0								
278.	28.66	-5.47	0	28.66	-5.47	0								
279.	29.66	-5.47	0	29.66	-5.47	0								
280.	30.66	-5.47	0	30.66	-5.47	0								
281.	31.66	-5.47	0	31.66	-5.47	0								
282.	32.66	-5.47	0	32.66	-5.47	0								

283.	33.66	-5.47	0	33.66	-5.47	0									
284.	34.66	-5.47	0	34.66	-5.47	0									
285.	35.66	-5.47	0	35.66	-5.47	0									
286.	36.66	-5.47	0	36.66	-5.47	0									
287.	37.66	-5.47	0	37.66	-5.47	0									
288.	38.66	-5.47	0	38.66	-5.47	0									
289.	39.66	-5.47	0	39.66	-5.47	0									
290.	40.66	-5.47	0	40.66	-5.47	0									
291.	41.66	-5.47	0	41.66	-5.47	0									
292.	42.66	-5.47	0	42.66	-5.47	0									
293.	43.66	-5.47	0	43.66	-5.47	0									
294.	44.66	-5.47	0	44.66	-5.47	0									
295.	45.66	-5.47	0	45.66	-5.47	0									
296.	46.66	-5.47	0	46.66	-5.47	0									
297.	47.66	-5.47	0	47.66	-5.47	0									
298.	48.66	-5.47	0	48.66	-5.47	0									
299.	49.66	-5.47	0	49.66	-5.47	0									
300.	50.66	-5.47	0	50.66	-5.47	0									
301.	51.66	-5.47	0	51.66	-5.47	0									
302.	52.66	-5.47	0	52.66	-5.47	0									
303.	53.66	-5.47	0	53.66	-5.47	0									
304.	54.66	-5.47	0	54.66	-5.47	0									
305.	55.66	-5.47	0	55.66	-5.47	0									

306.	-13.34	-6.47	0	-13.34	-6.47	0								
307.	-12.34	-6.47	0	-12.34	-6.47	0								
308.	-11.34	-6.47	0	-11.34	-6.47	0								
309.	-10.34	-6.47	0	-10.34	-6.47	0								
310.	-9.34	-6.47	0	-9.34	-6.47	0								
311.	-8.34	-6.47	0	-8.34	-6.47	0								
312.	-7.34	-6.47	0	-7.34	-6.47	0								
313.	-6.34	-6.47	0	-6.34	-6.47	0								
314.	-5.34	-6.47	0	-5.34	-6.47	0								
315.	-4.34	-6.47	0	-4.34	-6.47	0								
316.	-3.34	-6.47	0	-3.34	-6.47	0								
317.	-2.34	-6.47	0	-2.34	-6.47	0								
318.	-1.34	-6.47	0	-1.34	-6.47	0								
319.	-0.34	-6.47	0	-0.34	-6.47	0								
320.	0.66	-6.47	0	0.66	-6.47	0								
321.	1.66	-6.47	0	1.66	-6.47	0								
322.	2.66	-6.47	0	2.66	-6.47	0								
323.	3.66	-6.47	0	3.66	-6.47	0								
324.	4.66	-6.47	0	4.66	-6.47	0								
325.	5.66	-6.47	0	5.66	-6.47	0								
326.	6.66	-6.47	0	6.66	-6.47	0								
327.	7.66	-6.47	0	7.66	-6.47	0								
328.	8.66	-6.47	0	8.66	-6.47	0								

329.	9.66	-6.47	0	9.66	-6.47	0								
330.	10.66	-6.47	0	10.66	-6.47	0								
331.	11.66	-6.47	0	11.66	-6.47	0								
332.	12.66	-6.47	0	12.66	-6.47	0								
333.	13.66	-6.47	0	13.66	-6.47	0								
334.	14.66	-6.47	0	14.66	-6.47	0								
335.	15.66	-6.47	0	15.66	-6.47	0								
336.	16.66	-6.47	0	16.66	-6.47	0								
337.	17.66	-6.47	0	17.66	-6.47	0								
338.	18.66	-6.47	0	18.66	-6.47	0								
339.	19.66	-6.47	0	19.66	-6.47	0								
340.	20.66	-6.47	0	20.66	-6.47	0								
341.	21.66	-6.47	0	21.66	-6.47	0								
342.	22.66	-6.47	0	22.66	-6.47	0								
343.	23.66	-6.47	0	23.66	-6.47	0								
344.	24.66	-6.47	0	24.66	-6.47	0								
345.	25.66	-6.47	0	25.66	-6.47	0								
346.	26.66	-6.47	0	26.66	-6.47	0								
347.	27.66	-6.47	0	27.66	-6.47	0								
348.	28.66	-6.47	0	28.66	-6.47	0								
349.	29.66	-6.47	0	29.66	-6.47	0								
350.	30.66	-6.47	0	30.66	-6.47	0								
351.	31.66	-6.47	0	31.66	-6.47	0								

352.	32.66	-6.47	0	32.66	-6.47	0								
353.	33.66	-6.47	0	33.66	-6.47	0								
354.	34.66	-6.47	0	34.66	-6.47	0								
355.	35.66	-6.47	0	35.66	-6.47	0								
356.	36.66	-6.47	0	36.66	-6.47	0								
357.	37.66	-6.47	0	37.66	-6.47	0								
358.	38.66	-6.47	0	38.66	-6.47	0								
359.	39.66	-6.47	0	39.66	-6.47	0								
360.	40.66	-6.47	0	40.66	-6.47	0								
361.	41.66	-6.47	0	41.66	-6.47	0								
362.	42.66	-6.47	0	42.66	-6.47	0								
363.	43.66	-6.47	0	43.66	-6.47	0								
364.	44.66	-6.47	0	44.66	-6.47	0								
365.	45.66	-6.47	0	45.66	-6.47	0								
366.	46.66	-6.47	0	46.66	-6.47	0								
367.	47.66	-6.47	0	47.66	-6.47	0								
368.	48.66	-6.47	0	48.66	-6.47	0								
369.	49.66	-6.47	0	49.66	-6.47	0								
370.	50.66	-6.47	0	50.66	-6.47	0								
371.	51.66	-6.47	0	51.66	-6.47	0								
372.	52.66	-6.47	0	52.66	-6.47	0								
373.	53.66	-6.47	0	53.66	-6.47	0								
374.	54.66	-6.47	0	54.66	-6.47	0								

375.	55.66	-6.47	0	55.66	-6.47	0							
376.	-13.34	-7.47	0	-13.34	-7.47	0							
377.	-12.34	-7.47	0	-12.34	-7.47	0							
378.	-11.34	-7.47	0	-11.34	-7.47	0							
379.	-10.34	-7.47	0	-10.34	-7.47	0							
380.	-9.34	-7.47	0	-9.34	-7.47	0							
381.	-8.34	-7.47	0	-8.34	-7.47	0							
382.	-7.34	-7.47	0	-7.34	-7.47	0							
383.	-6.34	-7.47	0	-6.34	-7.47	0							
384.	-5.34	-7.47	0	-5.34	-7.47	0							
385.	-4.34	-7.47	0	-4.34	-7.47	0							
386.	-3.34	-7.47	0	-3.34	-7.47	0							
387.	-2.34	-7.47	0	-2.34	-7.47	0							
388.	-1.34	-7.47	0	-1.34	-7.47	0							
389.	-0.34	-7.47	0	-0.34	-7.47	0							
390.	0.66	-7.47	0	0.66	-7.47	0							
391.	1.66	-7.47	0	1.66	-7.47	0							
392.	2.66	-7.47	0	2.66	-7.47	0							
393.	3.66	-7.47	0	3.66	-7.47	0							
394.	4.66	-7.47	0	4.66	-7.47	0							
395.	5.66	-7.47	0	5.66	-7.47	0							
396.	6.66	-7.47	0	6.66	-7.47	0							
397.	7.66	-7.47	0	7.66	-7.47	0							

398.	8.66	-7.47	0	8.66	-7.47	0							
399.	9.66	-7.47	0	9.66	-7.47	0							
400.	10.66	-7.47	0	10.66	-7.47	0							
401.	11.66	-7.47	0	11.66	-7.47	0							
402.	12.66	-7.47	0	12.66	-7.47	0							
403.	13.66	-7.47	0	13.66	-7.47	0							
404.	14.66	-7.47	0	14.66	-7.47	0							
405.	15.66	-7.47	0	15.66	-7.47	0							
406.	16.66	-7.47	0	16.66	-7.47	0							
407.	17.66	-7.47	0	17.66	-7.47	0							
408.	18.66	-7.47	0	18.66	-7.47	0							
409.	19.66	-7.47	0	19.66	-7.47	0							
410.	20.66	-7.47	0	20.66	-7.47	0							
411.	21.66	-7.47	0	21.66	-7.47	0							
412.	22.66	-7.47	0	22.66	-7.47	0							
413.	23.66	-7.47	0	23.66	-7.47	0							
414.	24.66	-7.47	0	24.66	-7.47	0							
415.	25.66	-7.47	0	25.66	-7.47	0							
416.	26.66	-7.47	0	26.66	-7.47	0							
417.	27.66	-7.47	0	27.66	-7.47	0							
418.	28.66	-7.47	0	28.66	-7.47	0							
419.	29.66	-7.47	0	29.66	-7.47	0							
420.	30.66	-7.47	0	30.66	-7.47	0							

421.	31.66	-7.47	0	31.66	-7.47	0								
422.	32.66	-7.47	0	32.66	-7.47	0								
423.	33.66	-7.47	0	33.66	-7.47	0								
424.	34.66	-7.47	0	34.66	-7.47	0								
425.	35.66	-7.47	0	35.66	-7.47	0								
426.	36.66	-7.47	0	36.66	-7.47	0								
427.	37.66	-7.47	0	37.66	-7.47	0								
428.	38.66	-7.47	0	38.66	-7.47	0								
429.	39.66	-7.47	0	39.66	-7.47	0								
430.	40.66	-7.47	0	40.66	-7.47	0								
431.	41.66	-7.47	0	41.66	-7.47	0								
432.	42.66	-7.47	0	42.66	-7.47	0								
433.	43.66	-7.47	0	43.66	-7.47	0								
434.	44.66	-7.47	0	44.66	-7.47	0								
435.	45.66	-7.47	0	45.66	-7.47	0								
436.	46.66	-7.47	0	46.66	-7.47	0								
437.	47.66	-7.47	0	47.66	-7.47	0								
438.	48.66	-7.47	0	48.66	-7.47	0								
439.	49.66	-7.47	0	49.66	-7.47	0								
440.	50.66	-7.47	0	50.66	-7.47	0								
441.	51.66	-7.47	0	51.66	-7.47	0								
442.	52.66	-7.47	0	52.66	-7.47	0								
443.	53.66	-7.47	0	53.66	-7.47	0								

444.	54.66	-7.47	0	54.66	-7.47	0								
445.	55.66	-7.47	0	55.66	-7.47	0								
446.	-13.34	-8.47	0	-13.34	-8.47	0								
447.	-12.34	-8.47	0	-12.34	-8.47	0								
448.	-11.34	-8.47	0	-11.34	-8.47	0								
449.	-10.34	-8.47	0	-10.34	-8.47	0								
450.	-9.34	-8.47	0	-9.34	-8.47	0								
451.	-8.34	-8.47	0	-8.34	-8.47	0								
452.	-7.34	-8.47	0	-7.34	-8.47	0								
453.	-6.34	-8.47	0	-6.34	-8.47	0								
454.	-5.34	-8.47	0	-5.34	-8.47	0								
455.	-4.34	-8.47	0	-4.34	-8.47	0								
456.	-3.34	-8.47	0	-3.34	-8.47	0								
457.	-2.34	-8.47	0	-2.34	-8.47	0								
458.	-1.34	-8.47	0	-1.34	-8.47	0								
459.	-0.34	-8.47	0	-0.34	-8.47	0								
460.	0.66	-8.47	0	0.66	-8.47	0								
461.	1.66	-8.47	0	1.66	-8.47	0								
462.	2.66	-8.47	0	2.66	-8.47	0								
463.	3.66	-8.47	0	3.66	-8.47	0								
464.	4.66	-8.47	0	4.66	-8.47	0								
465.	5.66	-8.47	0	5.66	-8.47	0								
466.	6.66	-8.47	0	6.66	-8.47	0								

467.	7.66	-8.47	0	7.66	-8.47	0								
468.	8.66	-8.47	0	8.66	-8.47	0								
469.	9.66	-8.47	0	9.66	-8.47	0								
470.	10.66	-8.47	0	10.66	-8.47	0								
471.	11.66	-8.47	0	11.66	-8.47	0								
472.	12.66	-8.47	0	12.66	-8.47	0								
473.	13.66	-8.47	0	13.66	-8.47	0								
474.	14.66	-8.47	0	14.66	-8.47	0								
475.	15.66	-8.47	0	15.66	-8.47	0								
476.	16.66	-8.47	0	16.66	-8.47	0								
477.	17.66	-8.47	0	17.66	-8.47	0								
478.	18.66	-8.47	0	18.66	-8.47	0								
479.	19.66	-8.47	0	19.66	-8.47	0								
480.	20.66	-8.47	0	20.66	-8.47	0								
481.	21.66	-8.47	0	21.66	-8.47	0								
482.	22.66	-8.47	0	22.66	-8.47	0								
483.	23.66	-8.47	0	23.66	-8.47	0								
484.	24.66	-8.47	0	24.66	-8.47	0								
485.	25.66	-8.47	0	25.66	-8.47	0								
486.	26.66	-8.47	0	26.66	-8.47	0								
487.	27.66	-8.47	0	27.66	-8.47	0								
488.	28.66	-8.47	0	28.66	-8.47	0								
489.	29.66	-8.47	0	29.66	-8.47	0								

490.	30.66	-8.47	0	30.66	-8.47	0								
491.	31.66	-8.47	0	31.66	-8.47	0								
492.	32.66	-8.47	0	32.66	-8.47	0								
493.	33.66	-8.47	0	33.66	-8.47	0								
494.	34.66	-8.47	0	34.66	-8.47	0								
495.	35.66	-8.47	0	35.66	-8.47	0								
496.	36.66	-8.47	0	36.66	-8.47	0								
497.	37.66	-8.47	0	37.66	-8.47	0								
498.	38.66	-8.47	0	38.66	-8.47	0								
499.	39.66	-8.47	0	39.66	-8.47	0								
500.	40.66	-8.47	0	40.66	-8.47	0								
501.	41.66	-8.47	0	41.66	-8.47	0								
502.	42.66	-8.47	0	42.66	-8.47	0								
503.	43.66	-8.47	0	43.66	-8.47	0								
504.	44.66	-8.47	0	44.66	-8.47	0								
505.	45.66	-8.47	0	45.66	-8.47	0								
506.	46.66	-8.47	0	46.66	-8.47	0								
507.	47.66	-8.47	0	47.66	-8.47	0								
508.	48.66	-8.47	0	48.66	-8.47	0								
509.	49.66	-8.47	0	49.66	-8.47	0								
510.	50.66	-8.47	0	50.66	-8.47	0								
511.	51.66	-8.47	0	51.66	-8.47	0								
512.	52.66	-8.47	0	52.66	-8.47	0								

513.	53.66	-8.47	0	53.66	-8.47	0							
514.	54.66	-8.47	0	54.66	-8.47	0							
515.	55.66	-8.47	0	55.66	-8.47	0							

OptimizationOutputForm   — □ ×

The Optimium crane location is (23.66,-3.47,0) .

The Critical Weight is 17.48 Ton, with ID 2, demand Locaton of (-5.64,13.49,0)
and a lifting radius of 33.85 m.

The Critical Radius is 35.91.

Clearance of 0 m was assigned and considered for selecting the supply locations.

Total time of lifting operations neglecting hooking, unhooking and aligning of the weight is 147.22 min.

Total Cost is $282.85.

Below is a list of each demand location assigned to a pick location:

| Set Locations	Pick Locations
(-5.64,17.3,0)	(-4.34,2.53,0)
(-5.64,13.49,0)	(1.66,-3.47,0)
(-2.74,10.24,0)	(-4.34,3.53,0)
(-2.74,7.34,0)	(-2.34,-3.47,0)
(2.13,5.03,0)	(7.66,-3.47,0)
(5.89,5.03,0)	(7.66,-3.47,0)
(9.6,5.03,0)	(11.66,-3.47,0)
(13.72,5.03,0)	(15.66,-3.47,0)
(17.37,5.03,0)	(15.66,-3.47,0)
(20.62,5.03,0)	(14.66,-3.47,0)
(24.28,5.03,0)	(31.66,-3.47,0)
(28.4,5.03,0)	(29.66,-3.47,0)
(32.11,5.03,0)	(30.66,-3.47,0)
(35.99,5.26,0)	(34.66,-3.47,0)
(40.18,5.26,0)	(38.66,-3.47,0)
(43.84,5.26,0)	(41.66,-3.47,0)
(49.45,2.74,0)	(44.66,-3.47,0)
(49.45,6.65,0)	(47.66,-3.47,0)
(49.45,10.06,0)	(48.66,-3.47,0)
(49.45,13.72,0)	(49.66,-3.47,0)
(49.45,17.48,0)	(51.66,-3.47,0)
(43.84,14.55,0)	(45.66,-3.47,0)
(40.18,14.55,0)	(41.66,-3.47,0)
(35.99,14.55,0)	(38.66,-3.47,0)
(32.11,13.16,0)	(34.66,-3.47,0)
(28.4,13.16,0)	(32.66,-3.47,0)
(19,18.16,0)	(10.66,-3.47,0)
(19,13.16,0)	(7.66,-3.47,0)
(19,8.16,0)	(11.66,-3.47,0)
(9.6,13.16,0)	(8.66,-3.47,0)
(5.89,13.16,0)	(4.66,-3.47,0)
(2.13,13.16,0)	(3.66,-3.47,0)

Fig 17. Automatic output of the capacity/time optimization

83

Table 3 Case Study 1 results for different capacity/-time weights

Capacity-Time percentage	Critical Moment (t.m.)	Max. Lifting Radius (m.)	Total Time (min.)	Total cost ($)
0 %– 100 %	826.79	68.184	57.46	110.16
10 % – 90 %	689.59	39.46	100	191.14
20 %-80 %	615.64	37.31	115.26	221.34
50 %-50 %	591.72	35.91	147	282.44
80 %-20 %	591.72	35.91	247.86	476
90 %-10 %	591.72	35.91	321.98	642.94
100 %-0 %	576.66	35.1	487.22	935

Following implementation of the moment/-time optimization and allocation of the tower crane position and material supply locations, the wind analysis was implemented. The tower crane legs reactions were calculated and the mast horizontal deflection hinging on the maximum foreseeable wind speed. Prior to that, the web scraping code was applied on one of the well-known weather forecasting websites (Wunderground.com) which contains historical data, to extract the wind information on an hourly basis for five years.

The objective is to collect all of the published information about a certain location (in this case New York, since it was chosen for the case study) in one CSV file, which saves a remarkable amount of time for the user. A generated CSV file contains approximately 52,000 rows of wind behavior each hour for 5 years. This detailed information can be utilized for tower crane operation management; however, our main target is the maximum wind speed for worst case scenario predictions. Fig 18 depicts the various wind speeds and gusts. A wind gust is a sudden increase in wind speed. According to Shapiro and Shapiro [93], in the US, gusts are adopted as a 3 s interval,

but for the sake of simplicity, and to magnify the safety precautions, wind gusts were considered as an alternative. The highest wind gust monitored was 32 m/s.
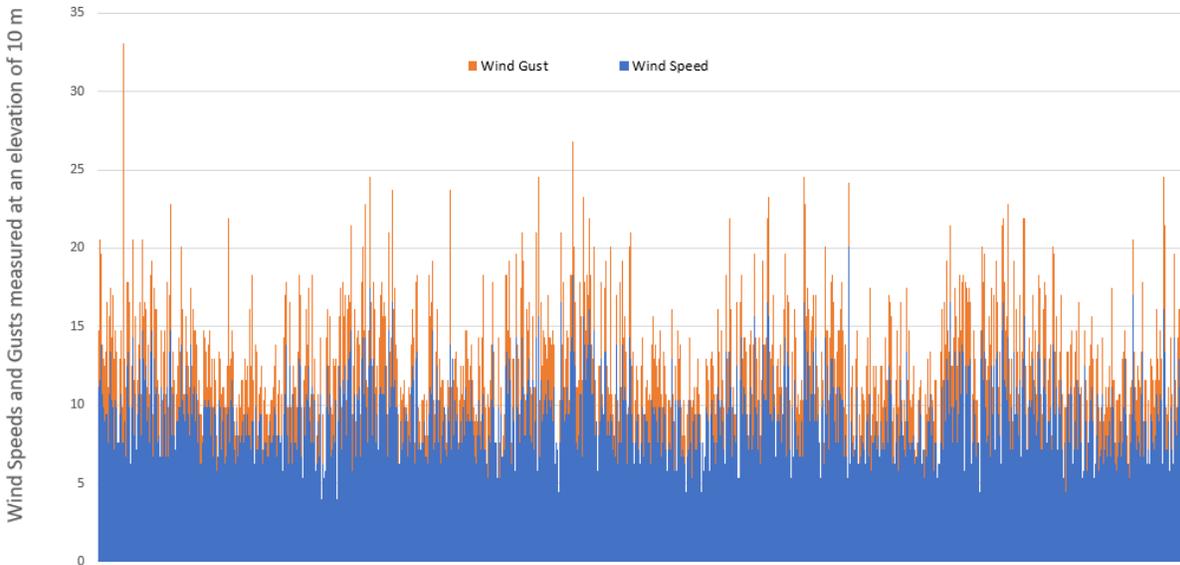

Fig 18. Hourly Wind Speeds and Gusts for the Last Five Years in New York City

Adopting the case of 50/50% weight ratios for the moment and time operation, respectively. Fig 17 shows that the maximum moment observed was when maneuvering the module no. 2 which has a weight of 17.48 t, a value of 603.89 t.m accompannied with a pick and set distances of 22 m and 33.85 m, and the maximum lift radius is 35.91 m. This data helped to inform the tower crane model selection procedure. Considiring the aforementioned values from Fig 17, a 50 ton Liebherr 1250-HC was assigned a capacity of 23 t. over a maximum lifting radius of 50.5 m. (Fig 19 shows different configurations of Liebherr 1250 HC 50).
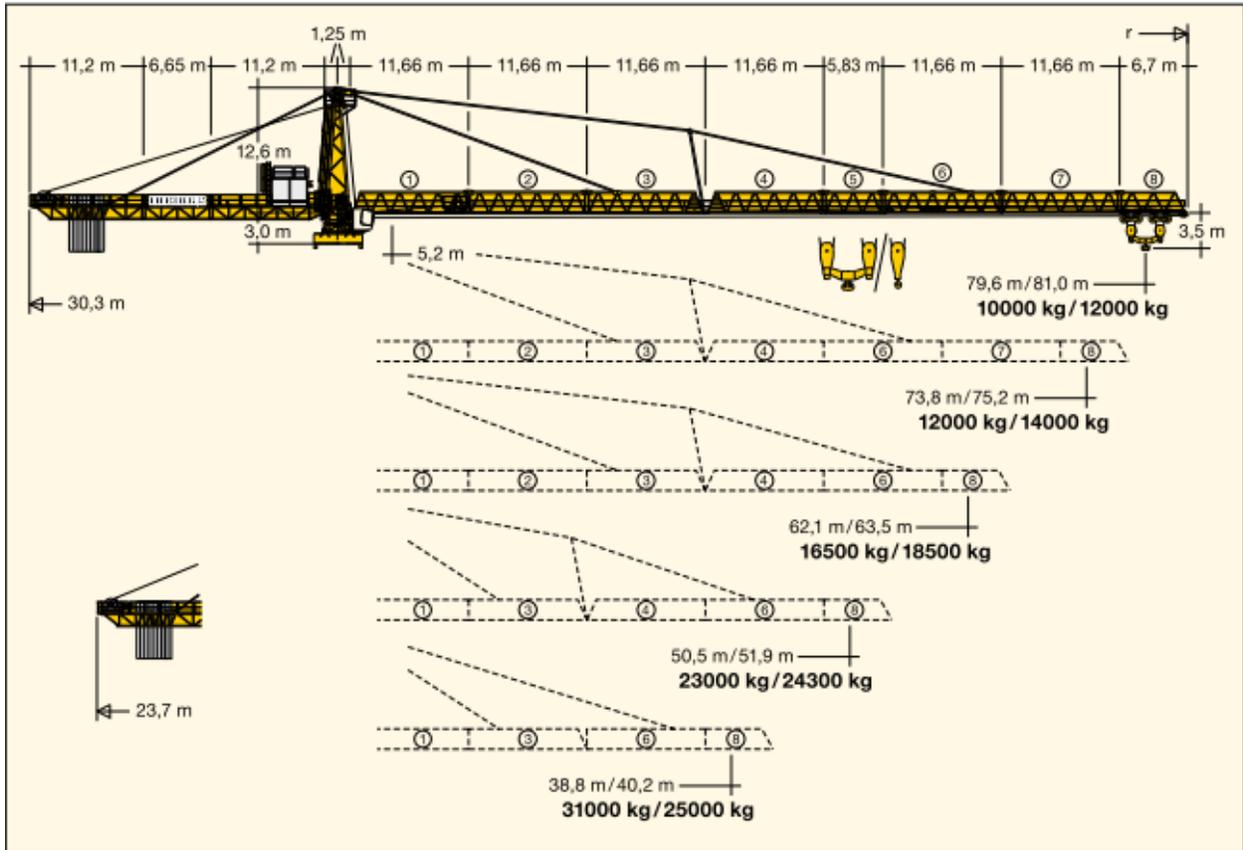
Fig 19. Liebherr 1250 HC 50 Jib configurations, (republished with consent)

The clearance between the crane and supply locations, it should be noted, was not considered, given that the case was hypothetical, and the wind analysis was the primary objective. The output screen in Fig 20 notifies the user using a red-colored alert when the stability of the tower crane is being threatened by high wind speeds (32 m/s, which is the maximum potential wind gust was found in the past 5 years histoircal wind data of New York city) meaning that, a change in ballast base dimensions is required. As shown in the figure, this was substantiated in this case by the fact that two of the four tower crane legs had negative pressures (-88 kPa), reflecting a contactless state of two legs to the ground; neverthless those reactions were calculated in case of a jib swinging angles of 0° to the north.

Naturally, wind can apply pressure from any direction, and a tower crane hasd 360° of jib swinging angle; for this reason, the automatic plots on the left side of Fig 20 is essential. The first plot of the five plots on the left side of Fig 20 represents the four legs reactions contingent upon a wind direction of 0° to the north simulating all angular positions of the jib. The other four plots represent the respective reactions to wind directions to the north (0°, 90°, 180°, 270°). AS shown, the five plots cover all possible scenarios of the wind and jib swinging angles. As shown in the figure, all five plots were found to have negative values confirming that the buffeted tower crane has no resistance.

Increasing the ballast base height from 1.8 to 2.5 m was found to generate four positive reactions. nonetheless, the computer program still generates an alert in such a case, the tower crane will still overturn in the presence of 32 m/s wind speed since there are negative values in different wind and jib directions situations, as presented in Fig 21 A ballast base height of 3 m was found to result in a green message (see Fig 22) shows the software reporting a safe erection of the tower crane mast against potential extreme wind speeds of 32 m/s wind speed since there are no negative values in any of the ground pressures plot. Moreover, total deflection in the presence of the wind is estimated.

Fig 22 represents the software reporting a safe erection of the tower crane with defelection of 0.03 m which is within the bounds of what is considered an acceptably safe range of deflection (0.08 m, 0.02 m). Fig 20, Fig 21 and Fig 22 show similar deflection results. Mast deformation, it should be noted, was determined based on the parameters in Equations (22) to (26) as described previously, and no tower configuration replacement was done, as the induced deflection was found to be within acceptable limits.

Table 4. Liebherr 1250 HC 50 Data for Performing the Wind Analysis

Liebherr 1250 HC 50 configurations		
Structure	Counterweight	75000 kg
	Total load	247510 kg
Wind	Speed	32 m/s
Outriggers	Longitudinal Distance	4 m
	Transversal Distance	4 m
Jib	Height	72.6 m
	Cross-Section	229.35 m^2
	Weight	27870 kg
Mast	Height	85.2 m
	Cross-Section	340.8 m^2
	Weight	138870 kg
	Member Width	30 cm
	Surface Area Width	4 m
Jib Section 1	Distance to CG	6.55 m
Jib Section 2	Distance to CG	18.15 m
Jib Section 3	Distance to CG	29.75 m
Jib Section 4	Distance to CG	41.35 m
Jib Tip	Distance to CG	50.5 m
Counter-jib	Distance to CG	15.6 m
Counterweight	Distance to CG	29.8 m
Critical load	Weight	17500 KG

	Lifting Radius	33.85 m
Ballast Base	Length	12 m
	Width	12 m
	Height	1.6 m

The tower crane is unstable against over tipping in the presence of max potential wind velocity of 32m/s

The dimensions of the ballast base must be increased.
The Tower crane leg pressures are mentioned below in case of swing angle of 0 and wind angle from the north of 0

Grounding pressure on the right frontal tower crane leg (Pfb) = 1106.02 Kpa.
Grounding pressure on the left frontal tower crane leg (Pfc) = 1106.02 Kpa.
Grounding pressure on the right frontal tower crane leg(Prb) = -88 KPa.
Grounding pressure on the right frontal tower crane leg(Prc) = -88 KPa.

The total deflection of the mast in case of an out of service condition at speed of 32 (m/s) is 0.03 (m).
The tower crane is safe against the maximum potential gust speeds in this area, the allowable value of the mast deflection is 0.02 (m) in case of normal safety procedures and 0.08 (m) in case of conservative safety procedures.

Fig 20. Automatic wind analysis output of the computer program regarding the Liebherr 1250 HC 50
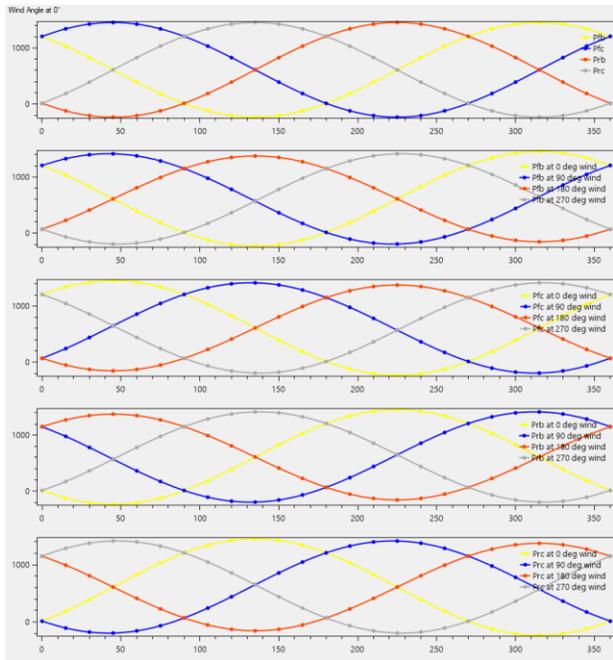
The tower crane is unstable against over tipping in the presence of max potential wind velocity of 32m/s

The dimensions of the ballast base must be increased.
The Tower crane leg pressures are mentioned below in case of swing angle of 0 and wind angle from the north of 0

Grounding pressure on the right frontal tower crane leg (Pfb) = 1208.08 Kpa.
Grounding pressure on the left frontal tower crane leg (Pfc) = 1208.08 Kpa.
Grounding pressure on the right frontal tower crane leg(Prb) = 14.06 KPa.
Grounding pressure on the right frontal tower crane leg(Prc) = 14.06 KPa.

The total deflection of the mast in case of an out of service condition at speed of 32 (m/s) is 0.03 (m).
The tower crane is safe against the maximum potential gust speeds in this area, the allowable value of the mast deflection is 0.02 (m) in case of normal safety procedures and 0.08 (m) in case of conservative safety procedures.

Fig 21. Output of the Computer Program after increasing the height of the ballast base to 2.5 m
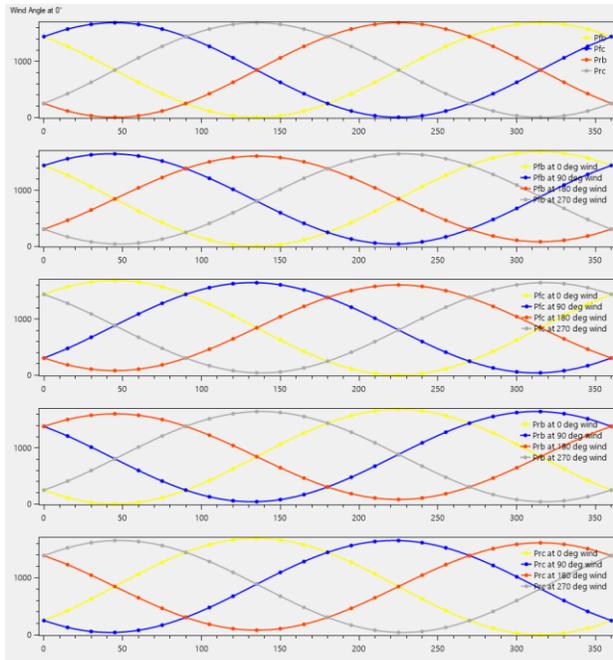
The tower crane is stable against over tipping in the presence of max potential wind velocity of 32m/s
The Tower crane leg pressures are mentioned below in case of swing angle of 0 and wind angle from the north of 0

Grounding pressure on the right frontal tower crane leg (Pfb) = 1444.49 Kpa.
Grounding pressure on the left frontal tower crane leg (Pfc) = 1444.49 Kpa.
Grounding pressure on the right frontal tower crane leg(Prb) = 250.48 KPa.
Grounding pressure on the right frontal tower crane leg(Prc) = 250.48 KPa.

The total deflection of the mast in case of an out of service condition at speed of 32 (m/s) is 0.03 (m).
The tower crane is safe against the maximum potential gust speeds in this area, the allowable value of the mast deflection is 0.02 (m) in case of normal safety procedures and 0.08 (m) in case of conservative safety procedures.

Fig 22. Output of the computer program after increasing the height of the ballast base to 3 m

4.2 Nadoushani et al. [82] Numerical Exemplary:

To demonstrate the efficiency of the mathematical optimization, the case study presented by Nadoushani et al. [82] was selected for implementation of the methodology. In Nadoushani et al. [82] case study, the construcation site contained 6 potential crane locations, 6 potential material supply locations and 10 material destinations (see Table 8 and Table 9). The same parameters from the previous case study were followed for the tower cranes velcotites and travel hook coordination. The cost information from Nadoushani et al. [82] (rental and operating cost table) was found to demonstrate a directional propornality of the crane capacity to the operational and renting cost; moreover, rental costs were found to be comparatively higher than operational costs, a finding which conceptually links lower costs with a greater weight assigned to safety and lower crane capacity (see Table 5). Therefore, the optimal the total cost was achieved by locating the material supply location closer to the crane location.

In this repsect, 80% and 20% of safety and operation time percentages were assigned, respectively. The number of potential coordintes of crane and supply location, it should be noted, was relatively small; as such, a higher safety weight yielded to similar results. Fig 23 depicts the scatterplot generated from the computer code of the construction site coordinates provided, demonstrating the optimal crane and material supply locations and material desitnations.

Fig 23. Automatically generated plot of the site layout coordinates including the optimum crane and supply location and demand locations

Table 6 and Table 7 preview, meanwhile, provide further details on some of the outputs of the computer program. Similarly to with Nadoushani case study, the same crane location was selected. On the other hand, two supply locations only were selected instead of three since our algorithm wants to minimze transportation distance as possible because of the heigher percentage was assigned to the lifting moments; crane capacity, ultimately safety. Moreover the algorithm set about matching a pick location for each demand location in a different manner than the Nadoushani et al. study, which provided supply locations without assigning demand locations when integrating crane capacity. The maximum moment imposed on the crane in the Nadoushai solution was 431 t.m. pointing to the selection of the 450 t.m. accomapnied with rental and operating costs of 2.7 and 1.9 (AUD/min), respectively. In contrast, the developed model outputed a critical lifting moment of 165.8. t.m. resulting into selection of a lower crane capacity (the 200 t.m) with a rental

cost of 1.2 (AUD/min) and operating cost of 0.9 (AUD/min), respecitvely. However, a total cost comparison was not feasible since, in the Nadoushani study, the number of material transported per block is not disclosed. However, a lower capacity crane implies cost reduction. Moreover, the propsed methodology directs decision makers toward safer crane operations if the tower crane model is already set.

Table 5 Tower Crane Rental and Operating Costs of Nadoushani et al. [82] case study

Crane Capacity (m.t.)	Rental Costs (AUD/min)	Operating Costs (AUD/min)
200	1.2	0.9
250	1.5	1.1
300	1.8	1.3
350	2.1	1.5
400	2.4	1.7
450	2.7	1.9
500	3	2.1
550	3.3	2.3
600	3.6	2.5
650	3.9	2.7
700	4.2	2.9

Table 6 Moment-Time Operation Optimization Outputs of Nadoushani et al. [82] case study

Crane Location	Module ID	Pick Location	$M_{i,1,k}{}^{O}$	$T^h_{(i,j,k)}$	$T^v_{(i,j,k)}$	$T_{(i,j,k)}$	Set-Distance	Pick-Distance
Cr_1 (11.25, -7.5, -4.2)	D_1	S_4	98.86	0.1843	0.9450	1.1293	25.16	32.40
	D_2	S_3	73.74	0.1773	0.8250	1.0023	16.77	15.91
	D_3	S_3	137.32	0.3503	0.7050	1.0553	31.82	15.91
	D_4	S_4	21.66	0.1730	0.6450	0.8180	27.48	32.40
	D_5	S_3	199.24	0.4906	0.1050	0.5956	10.61	15.91
	D_6	S_3	14.20	0.2723	0.0050	0.2773	8.39	15.91
	D_7	S_3	48.71	0.4071	0.0050	0.4121	34.57	15.91
	D_8	S_4	12.83	0.2197	0.1050	0.3247	25.75	32.40
	D_9	S_4	44.69	0.3872	0.1650	0.5522	13.73	32.40
	D_{10}	S_3	95.08	0.4856	0.2250	0.7106	39.15	15.91

Table 7 The developed methodology results juxtaposed to Nadoushani et al. [82] results

Outputs	Developed Study	Nadoushani et al [82]
Material transportation time (min)	128.44	609.31
Operating Costs (AUD)	115.6	1,157.7
Critical moment (m.t.)	165.8	431
Rental costs (AUD/min)	154.13	2.7
Total Costs	269.7	2,802.8
Feasible supply locations	S_3, S_4	S_3, S_4, S_5

Table 8 Potential Crane and Material Supply Locations Coordinates of Nadoushani et al. [82] case study

Point label	x coordinate	y coordinate	z coordinate
Cr_1	11.25	-7.5	-4.2
Cr_2	37.5	-24.925	-4.2
Cr_3	52.5	19	-4.2
Cr_4	-4.2	25.3	-4.2
Cr_5	37.5	-11.25	-4.2
Cr_6	52.5	5	-4.2
S_1	79	11.5	0
S_2	79	-25	0
S_3	22.5	-18.75	0
S_4	-15	11.5	0
S_5	11.25	38	0
S_6	48.76	38	0

Table 9 Lifted Material Destination Coordinates of Nadoushani et al. [82] case study

Point label	x coordinate	y coordinate	z coordinate	Lifted Module Weight (t)
D_1	0	15	56..7	2.41
D_2	26.25	0	49.5	3.19
D_3	33.75	15	42.3	3.86

D_4	6.7	19.6	38.7	0.51
D_5	3.75	0	6.3	10.42
D_6	18.75	-3.75	0.3	0.79
D_7	45	-15	0.3	1.28
D_8	11.25	18.25	6.3	0.31
D_9	3.75	4	9.9	1.27
D_{10}	48.75	-18.75	13.5	2.25

4.3 Dallas Tower Crane Failure:

A tower crane in Dallas, Texas, collapsed in June 2019. The structure failure occurred due to a recorded severe wind speeds of 32 m/s. The buffeted tower crane base did not overturn since it was guyed and fixed securely to the ground transferring all the dynamic forces to the fractured mast; a breakage was triggered by an over-limit horizontal deflection. The tower crane model in this case was a Terex Peiner SK 415-20, designed to withstand winds of up of 41 m/s. The tower crane failure occurred in the same direction as the wind.

Normally, a weathervane tower crane jib allows the wind to make its initial contact on the counterweight before reaching the jib tip, but this was not the case in the Dallas incident. Nevertheless, the proposed methodology can be applied to investigate the presence of over-limits horizontal deflection. According to Davenport [95], the suggested urban/suburban ratio of the Dallas area is 1/4. Jib and mast components and lengths were thus assumed accordingly and mast and jib lengths in contrast with remaining tower crane configurations which were following the Prier SK 415-20 manufacturer data. The tower crane was manufactured of structural steel (S35), (with a Young Modulus of) 210 GPa. Table 10 presents the aforementioned information.

The GUI of the developed tool, it should be noted, allows the user to input all the relevant data of the tower crane components as shown in Fig 24; quantity, length, width, height, weight, distance from the component CG to the tower crane CG and cross-section. The user can overlook any insignificant data with respect to the calculation of the ground bearing pressure reactions and horizontal deflection since they are interconnected, whereas the primary concern here is to single out the deflection. In this case, Fig 25 demonstrated a horizontal deflection of 0.2 m as previously mentioned and shown in *Fig 13*, triggered by the 32 m/s wind speed this deflection is higher than the conservative allowable deflection of 0.09 m and the normal allowable deflection of 0.19 m.

Notably, this procedure does not contemplate safety factors, dynamic forces, metallurgical investigations and vibrations induced due to natural frequency—criteria which add more restrictions to the allowable deflections and exacerbate the mast deflection. The methodology underscores the inadequacy of the Terex Peiner SK 415-20 tower crane to withstand wind speeds in excess of 31 m/s. Conceptually, this procedure can broaden the decision maker's frame of reference when selecting a tower crane model.

Table 10 Dallas Tower Crane Data for Performing the Wind Analysis

Terex Peiner SK 415-20 configurations		
Structure	Counterweight	36820 kg
	Total load	149019 kg
Wind	Speed	32 m/s
Outriggers	Longitudinal Distance	2.34 m
	Transversal Distance	2.34 m
Jib	Height	85.6 m

	Cross-Section	132 m^2
	Weight	12310 kg
Mast	Height	93.86
	Cross-Section	228 m^2
	Weight	79890 kg
	Member Width	28 cm
	Surface Area Width	2.43 m
Jib Section 1	Distance to CG	7.145 m
Jib Section 2	Distance to CG	19.425 m
Jib Section 3	Distance to CG	31.335 m
Jib Section 4	Distance to CG	40.1 m
Jib Section 5	Distance to CG	48 m
Jib Section 6	Distance to CG	59 m
Jib Tip	Distance to CG	65.1 m
Counter-jib	Distance to CG	-11 m
Counterweight	Distance to CG	22.3 m

Fig 24. Graphical user interface of the wind analysis tab

The tower crane is unstable against over tipping in the presence of max potential wind velocity of 32m/s

The dimensions of the ballast base must be increased (height).
The Tower crane leg pressures are mentioned below in case of swing angle of 0 and wind angle from the north of 0

Grounding pressure on the right frontal tower crane leg (Pfb) = 2074.82 Kpa.
Grounding pressure on the left frontal tower crane leg (Pfc) = 2074.82 Kpa.
Grounding pressure on the right frontal tower crane leg(Prb) = -2036.81 KPa.
Grounding pressure on the right frontal tower crane leg(Prc) = -2036.81 KPa.

The total deflection of the mast in case of an out of service condition at speed of 32 (m/s) is 0.2 (m).
The tower crane is safe against the maximum potential gust speeds in this area, the allowable value of the mast deflection is 0.19 (m) in case of normal safety procedures and 0.09 (m) in case of conservative safety procedures.

Chapter 5: Conclusion

This paper presented a new approach for processing the site layout quadratic combinatorial optimization problem. A mixed-generic mathematical approach was developed contemplating crane capacity and hook travel time as parameters for crane and supply locations selection. Distance-based-optimization technique was applied, enabling more efficient crane operations or lifting-moment minimized operations, where the latter tends the algorithm to minimize distances of hook displacement, accordingly, employing lower-capacity tower crane and decreasing the total cost.

The methodology was implemented on two case studies to investigate its practicability on both small- and large-scales construction sites. The case of large construction site with 514 available spots for crane and material supply was found to increase the complexity, with roughly 8.5 million permutations involved in selecting the optimum locations. The Nadoushani et al. [82] case study was adopted as a small scale construction site, resulting in considerable improvement with a maximum moment imposed of 165.8 t.m. Therefore, a crane capacity of 200 t.m. with a total costs of 2.1 (AUD/min) and substituting the Nadoushani et al. solution of a critical moment of 430 t.m. accordingly, selecting 450 t.m. crane with the 4.7 (AUD/min).

Moreover, a static wind analysis was conducted to provide more dimensionality of security for the evaluation of the selected tower crane model and the erection configurations. This simplistic approach enriches the decision maker's understanding of the ability of a given tower crane to withstand extreme wind speeds which can ascertained based on wind speed data from specific

locations over a long period of time. The first case study demonstrated the effectiveness of the proposed methodology with respect to the selected tower crane model, contingent upon data from the first part of the methodology and anchor ballast base dimensions were also determined besides; moreover, the tower crane mast was examined statically and mathematically for horizontal deflection resistance.

The Dallas crane collapse was also investigated through the implementation of the mast horizontal deflection procedure, and the results generated showed that the tower crane model employed in that case was not sufficient to withstand wind speeds of at 32 m/s (and excessive mast deformation and failure occurred accordingly). It should be mentioned that the proposed analysis is not intended as substitute for manufacturers' tools for selecting and setting up the tower crane configurations. Nevertheless, it is a complementary procedure for augmenting the safety precautions. The developed methodology is represented in terms of a computer program with a user-friendly GUI for more flexibility and time-saving applications as an alternative to tedious and manual procedures.

Notation

x = coordinate along the x-axis.

y = coordinate along the y-axis.

z = coordinate along the z-axis.

s = One supply location of the accessible supply locations.

d = One demand location of the accessible demand locations.

c = One crane location of the accessible crane locations.

S = Supply location set inside the site area boundaries

D = Demand location set inside the site area boundaries.

C = Crane location set inside the site area boundaries.

x_c, y_c, z_c = Tower crane three dimensional coordinates installed at location c

x_s, y_s, z_s = Supply location coordinates of a location i.

x_d, y_d, z_d = Demand location coordinates of a location j.

W_{load} = weight of the payload with all the accessories (e.g. shackles, spreader bars, slings, hook, etc.).

d = Euclidean distance separating the center of mass of the payload and the center of the mast

M_{load} = Lifting moment exerted by a payload W_{load}.

k = weight of the payload.

$M_{k,s,c}$ = Lifting moment of moving a payload k between a crane location c and a supply location s.

$M_{k,d,c}$ = Lifting moment of moving a payload k between a crane location c and a demand location d.

M_{max} = Maximum lifting moment produced of moving a payload between the crane, supply and demand locations.

$R_{k,u,c}$ = Reach of the crane for a payload w_k picked (or dropped) at a point defined by (x_u, y_u) by a crane located at (x_c, y_c).

C_u = Constant represents the clearance between the crane base and material supply locations.

V_r = Trolley radial velocity (m/min)

V_ω = Jib slewing velocity (rad/min)

V_h = Hoist vertical velocity (m/min)

$L_{luffing}$ = Length of the luffing crane jib.

$T^\omega_{(s,d,c)}$ = Slewing hook travel time of a tower crane at location c from supply location s to a demand location d.

$T^v_{(s,d,c)}$ = Vertical hook travel time of a tower crane at location c from supply location s to a demand location d.

$T^r_{(s,d,c)}$ = Transversal hook travel time of a tower crane at location c from supply location s to a demand location d.

$T^h_{(s,d,c)}$ = Horinzontal hook travel time of a tower crane at location c from supply location s to a demand location d.

$T_{(s,d,c)}$ = Total hook travel time of a tower crane at location c from supply location s to a demand location d.

TC = Total cost of operating the tower crane.

α = Numerical value reflects the crane operator skill to coordinate between hook transversal and

slewing movements.

β = Numerical value reflects the crane operator skill to coordinate between hook horizontal and vertical movements.

γ_k = Numerical value reflects obstructions to maneuver the crane hook at a crane location k

p_m = Percentile value of the crane capacity weight in the optimization output.

p_t = Percentile value of the hook travel time weight in the optimization output.

$O_{k,s,d,c}$ = Weight of the twofold optimization of $M^o{}_{i,j,k}$ and

C_o^m = Operation cost of a tower crane of a type m

C_R = Rental cost of a tower crane of a type m

$M^o_{k,s,d,c}$ = The optimal value of the objective function between $M_{k,s,c}$ and $M_{k,d,c}$.

$T_{k,s,d,c}$ = The total time of moving a payload k between crane location c, supply location s and demand location d.

d_t = Distance between two anchor pins or base supports in the transverse direction (m)

d_l = Distance between two anchor pins or base supports in the longitudinal direction (m)

V_u = The total vertical weight of the crane, weight and all rigging accessories (KN).

α = The horizontal swinging angle.

v = Wind velocity at specific altitude (m/s).

$v_\circ$ = Wind velocity measured on an elevation of 10 m (m/s).

δ = AG. Davenport Power-low exponent

C_f = The ratio between the sum of the face areas of members in the frame and gross area enclosed by the borders of the frame

q_m = Wind pressure buffeting on the centroid of the mast (KN/m^2)

q_j = Wind pressure buffeting on the centroid of the jib (KN/m^2)

q_l = Wind pressure buffeting on the centroid of the lifted module (KN/m^2)

H_m = Vertical distance between ground level to half the height of the mast (m)

H_j = Vertical distance between ground level to the jib centroid (m)

H_l = Vertical distance between ground level to the module centroid (10 m)

M_u = Ultimate moment (KN.m)

M_w = Wind moment (KN.m)

A = Area of cross section exposed the wind (m^2)

F = Resultant force of wind pressure on areas of cross-section of crane components and lifted module (KN)

M_{ns} = Frontward or rearward moment (KN.m)

M_{nr} = Over the side moment (KN.m)

ω = Wind direction measured counterclockwise from the north

P_{fb} = Grounding pressure on the right frontal tower crane leg. (kPa)

P_{fc} = Grounding pressure on the left frontal tower crane leg (kPa)

P_{rb} = Grounding pressure on the right reared tower crane leg (kPa)

P_{rc} = Grounding pressure on the left reared tower crane leg (kPa)

δ_c = backward deflection of tower crane mast due to the counterweight (m)

M_c = rearward moment triggered by the counterweight and counter jib components weights (KN.m)

Q = Weight of the rotating parts on top of the mast additional to 1/3 of the mast weight (KN)

E = Young Modulus which is the measure of a solid material stiffness against deformation (GPa)

I = Moment of Inertia of the tower crane mast section (m^4)

σ = Wind force per unit length of the mast

δ_w = Frontward deflection of tower crane mast due to the buffeting wind.

W_w = Wind Force applied on the center of the over tower

References

[1] A. Shapira, B. Lyachin, B. Lyanchin, Identification and Analysis of Factors Affecting
     Safety on Construction Sites with Tower Cranes, 9364 (2009) 24–33.
     https://doi.org/10.1061/(ASCE)0733-9364(2009)135.

[2] P. Yow, R. R., F. K., Crane accidents 1997-1999: a report of the crane unit of the division
     of occupational safety and health, (n.d.).

[3] S. Peurifoy, A. Shapira, Construction Planning, Equipment and Methods, (2011).

[4] A. Shapira, G. Lucko, C.J. Schexnayder, Cranes for building construction projects, J.
     Constr. Eng. Manag. 133 (2007) 690–700. https://doi.org/10.1061/(ASCE)0733-
     9364(2007)133:9(690).

[5] X. Wang, H. Wang, D. Wu, Interactive simulation of crawler crane/s lifting based on
     OpenGL, Proc. ASME Des. Eng. Tech. Conf. 3 (2008) 1533–1540.
     https://doi.org/10.1115/DETC2008-49608.

[6] H.L. Guo, H. Li, V. Li, VP-based safety management in large-scale construction projects:
     A conceptual framework, Autom. Constr. 34 (2013) 16–24.
     https://doi.org/10.1016/j.autcon.2012.10.013.

[7] P. Swuste, A "normal accident" with a tower crane? An accident analysis conducted by
     the Dutch Safety Board, Saf. Sci. 57 (2013) 276–282.
     https://doi.org/10.1016/j.ssci.2013.03.002.

[8] W. Zhou, T. Zhao, W. Liu, J. Tang, Tower crane safety on construction sites: A complex

sociotechnical system perspective, Saf. Sci. 109 (2018) 95–108.

https://doi.org/10.1016/j.ssci.2018.05.001.

[9]   C. Zhao, J. Zhang, X. Zhong, J. Zeng, S. Chen, Analysis of accident safety risk of tower

        crane based on fishbone diagram and the analytic hierarchy process, Appl. Mech. Mater.

        127 (2012) 139–143. https://doi.org/10.4028/www.scientific.net/AMM.127.139.

[10]   D. Sarkar, S. Shah, Evaluating Tower Crane Safety Factors for a Housing Project through

        AHP, NICMAR – J. Constr. Manag. XXVII (2012) 61–70.

[11]   I.J. Shin, Factors that affect safety of tower crane installation/dismantling in construction

        industry, Saf. Sci. 72 (2014) 379–390. https://doi.org/10.1016/j.ssci.2014.10.010.

[12]   A. Shapira, M. Simcha, AHP-Based Weighting of Factors Affecting Safety on

        Construction Sites with Tower Cranes, 9364 (2016) 2–11.

        https://doi.org/10.1061/(ASCE)0733-9364(2009)135.

[13]   E.S. Kim, S.K. Choi, Failure analysis of connecting bolts in collapsed tower crane,

        Fatigue Fract. Eng. Mater. Struct. 36 (2013) 228–241. https://doi.org/10.1111/j.1460-

        2695.2012.01716.x.

[14]   N.D. Zrnić, S.M. Bošnjak, V.M. Gašić, M.A. Arsić, Z.D. Petković, Failure analysis of the

        tower crane counterjib, Procedia Eng. 10 (2011) 2238–2243.

        https://doi.org/10.1016/j.proeng.2011.04.370.

[15]   A.A. Marquez, P. Venturino, J.L. Otegui, Common root causes in recent failures of

        cranes, Eng. Fail. Anal. 39 (2014) 55–64.

        https://doi.org/10.1016/j.engfailanal.2014.01.012.

[16]   M.R. Alam, S.F. Hassan, M.A. Amin, K. Arif-Uz-Zaman, M.A. Karim, Failure Analysis
        of a Mobile Crane: A Case Study, J. Fail. Anal. Prev. 18 (2018) 545–553.
        https://doi.org/10.1007/s11668-018-0437-1.

[17]   S. Hwang, Ultra-wide band technology experiments for real-time prevention of tower
        crane collisions, Autom. Constr. 22 (2012) 545–553.
        https://doi.org/10.1016/j.autcon.2011.11.015.

[18]   Y. Li, C. Liu, Integrating field data and 3D simulation for tower crane activity monitoring
        and alarming, Autom. Constr. 27 (2012) 111–119.
        https://doi.org/10.1016/j.autcon.2012.05.003.

[19]   G. Lee, H.H. Kim, C.J. Lee, S. Il Ham, S.H. Yun, H. Cho, B.K. Kim, G.T. Kim, K. Kim,
        A laser-technology-based lifting-path tracking system for a robotic tower crane, Autom.
        Constr. 18 (2009) 865–874. https://doi.org/10.1016/j.autcon.2009.03.011.

[20]   A. Shapira, Y. Rosenfeld, I. Mizrahi, Vision system for tower cranes, J. Constr. Eng.
        Manag. 134 (2008) 320–332. https://doi.org/10.1061/(ASCE)0733-9364(2008)134:5(320).

[21]   H. Li, G. Chan, M. Skitmore, Multiuser virtual safety training system for tower crane
        dismantlement, J. Comput. Civ. Eng. 26 (2012) 638–647.
        https://doi.org/10.1061/(ASCE)CP.1943-5487.0000170.

[22]   J.E. Beavers, J.R. Moore, R. Rinehart, W.R. Schriver, Crane-related fatalities in the
        construction industry, J. Constr. Eng. Manag. 132 (2006) 901–910.
        https://doi.org/10.1061/(ASCE)0733-9364(2006)132:9(901).

[23]   V.W.Y. Tam, I.W.H. Fung, Tower crane safety in the construction industry: A Hong

Kong study, Saf. Sci. 49 (2011) 208–215. https://doi.org/10.1016/j.ssci.2010.08.001.

[24]   R. Isherwood, H. Ceng, H. Hill, Tower crane incidents worldwide, (2010).

[25]   S. Essaid, R. Ellis, J. Hanna, 107 killed in crane collapse at Mecca's Grand Mosque, (n.d.).

[26]   J. Fortin, Dallas Crane Collapse Kills 1 and Injures 5, Officials Say - The New York Times, (n.d.).

[27]   W.E. Rodriguez-Ramos, R.L. Francis, Single crane location optimization, J. Constr. Eng. Manag. 109 (1983) 387–397. https://doi.org/10.1061/(ASCE)0733-9364(1983)109:4(387).

[28]   C. Gray, J. Little, A systematic approach to the selection of an appropriate crane for a construction site, Constr. Manag. Econ. 3 (1985) 121–144. https://doi.org/10.1080/01446198500000010.

[29]   S. Furusaka, C. Gray, A model for the selection of the optimum crane for construction sites, Constr. Manag. Econ. 2 (1984) 157–176. https://doi.org/10.1080/01446198400000015.

[30]   Hanna, A. S., & Lotfallah, A Fuzzy logic approach to selection of cranes, J. Struct. Eng. 30 (1999) 215–224.

[31]   M. Al-Hussein, S. Alkass, O. Moselhi, Optimization algorithm for selection and on site location of mobile cranes, J. Constr. Eng. Manag. 131 (2005) 579–590. https://doi.org/10.1061/(ASCE)0733-9364(2005)131:5(579).

[32]   A. Sawhney, A. Mund, Adaptive probabilistic neural network-based crane type selection system, J. Constr. Eng. Manag. 128 (2002) 265–273.

https://doi.org/10.1061/(ASCE)0733-9364(2002)128:3(265).

[33]   C. Huang, C.K. Wong, Optimization of crane setup location and servicing schedule for urgent material requests with non-homogeneous and non-fixed material supply, Autom. Constr. 89 (2018) 183–198. https://doi.org/10.1016/j.autcon.2018.01.015.

[34]   X. Liu, D.H. Chan, B. Gerbrandt, Bearing capacity of soils for crawler cranes, Can. Geotech. J. 45 (2008) 1282–1302. https://doi.org/10.1139/T08-056.

[35]   S. Kim, J. Kim, D. Lee, S. Ryu, Automatic optimal design algorithm for the foundation of tower cranes, Autom. Constr. 20 (2011) 56–65. https://doi.org/10.1016/j.autcon.2010.07.004.

[36]   M. Al-Hussein, M. Athar Niaz, H. Yu, H. Kim, Integrating 3D visualization and simulation for tower crane operations on construction sites, Autom. Constr. 15 (2006) 554–562. https://doi.org/10.1016/j.autcon.2005.07.007.

[37]   S. Han, A. Bouferguene, M. Al-Hussein, U.R. Hermann, 3D-Based Crane Evaluation System for Mobile Crane Operation Selection on Modular-Based Heavy Construction Sites, J. Constr. Eng. Manag. 143 (2017) 1–12. https://doi.org/10.1061/(ASCE)CO.1943-7862.0001360.

[38]   H. Taghaddos, S. Abourizk, Y. Mohamed, U. Hermann, Simulation-based auction protocol for resource scheduling problems, J. Constr. Eng. Manag. 138 (2012) 31–42. https://doi.org/10.1061/(ASCE)CO.1943-7862.0000399.

[39]   H.R. Reddy, K. Varghese, Automated path planning for mobile crane lifts, Comput. Civ. Infrastruct. Eng. 17 (2002) 439–448. https://doi.org/10.1111/0885-9507.00005.

[40]   P.L. Sivakumar, K. Varghese, N. Ramesh Babu, Automated path planning of cooperative crane lifts using heuristic search, J. Comput. Civ. Eng. 17 (2003) 197–207. https://doi.org/10.1061/(ASCE)0887-3801(2003)17:3(197).

[41]   C. Zhang, A. Hammad, Multiagent approach for real-time collision avoidance and path replanning for cranes, J. Comput. Civ. Eng. 26 (2012) 782–794. https://doi.org/10.1061/(ASCE)CP.1943-5487.0000181.

[42]   J. Wang, X. Zhang, W. Shou, X. Wang, B. Xu, M.J. Kim, P. Wu, A BIM-based approach for automated tower crane layout planning, Autom. Constr. 59 (2015) 168–178. https://doi.org/10.1016/j.autcon.2015.05.006.

[43]   S.C. Kang, H.L. Chi, E. Miranda, Three-dimensional simulation and visualization of crane assisted construction erection processes, J. Comput. Civ. Eng. 23 (2009) 363–371. https://doi.org/10.1061/(ASCE)0887-3801(2009)23:6(363).

[44]   M. Al-Hussein, S. Alkass, O. Moselhi, D-CRANE: A database system for utilization of cranes, Can. J. Civ. Eng. 27 (2000) 1130–1138. https://doi.org/10.1139/l00-039.

[45]   A.S. Hanna, SELECTCRANE: An expert system for optimum crane selection, in: Comput. Civ. Eng., ASCE, 1994: pp. 958–963.

[46]   A. Warszawski, Expert systems for crane selection, Constr. Manag. Econ. 8 (1990) 179–190. https://doi.org/10.1080/01446199000000015.

[47]   W.C. Hornaday, J.T. Haas, J.T. O'Connor, T. Went, Computer-Aided Planning for Heavy Lifts, 119 (1994) 498–515.

[48]   M. Al-Hussein, S. Alkass, O. Moselhi, An algorithm for mobile crane selection and

location on construction sites, Constr. Innov. 1 (2001) 91–105.
https://doi.org/10.1108/14714170110814532.

[49] K. Tantisevi, B. Akinci, Simulation-based identification of possible locations for mobile cranes on construction sites, J. Comput. Civ. Eng. 22 (2008) 21–30. https://doi.org/10.1061/(ASCE)0887-3801(2008)22:1(21).

[50] D. Wu, Y. Lin, X. Wang, X. Wang, S. Gao, Algorithm of crane selection for heavy lifts, J. Comput. Civ. Eng. 25 (2011) 57–65. https://doi.org/10.1061/(ASCE)CP.1943-5487.0000065.

[51] U. Hermann, A. Hendi, J. Olearczyk, M. Al-Hussein, An integrated system to select, position, and simulate mobile cranes for complex industrial projects, Constr. Res. Congr. 2010 Innov. Reshaping Constr. Pract. - Proc. 2010 Constr. Res. Congr. (2010) 267–276. https://doi.org/10.1061/41109(373)27.

[52] H. Safouhi, M. Mouattamid, U. Hermann, A. Hendi, An algorithm for the calculation of feasible mobile crane position areas, Autom. Constr. 20 (2011) 360–367. https://doi.org/10.1016/j.autcon.2010.11.006.

[53] J. Olearczyk, M. Al-Hussein, A. Bouferguène, Evolution of the crane selection and on-site utilization process for modular construction multilifts, Autom. Constr. 43 (2014) 59–72. https://doi.org/10.1016/j.autcon.2014.03.015.

[54] P. Sorokin, A. Mishin, V. Antsev, A. Red'Kin, System of providing sustainability of tower cranes from overturn in extreme wind loads, MATEC Web Conf. 224 (2018) 1–7. https://doi.org/10.1051/matecconf/201822402086.

[55] C. Klinger, Failures of cranes due to wind induced vibrations, Eng. Fail. Anal. 43 (2014) 198–220. https://doi.org/10.1016/j.engfailanal.2013.12.007.

[56] B. Ross, B. McDonald, S.E. Vijay Saraf, Big blue goes down. The Miller Park crane accident, Eng. Fail. Anal. 14 (2007) 942–961. https://doi.org/10.1016/j.engfailanal.2006.12.002.

[57] W. Chen, X. Qin, Z. Yang, P. Zhan, Wind-induced tower crane vibration and safety evaluation, J. Low Freq. Noise Vib. Act. Control. (2019) 1–16. https://doi.org/10.1177/1461348419847306.

[58] M.H. El Ouni, N. Ben Kahla, S. Islam, M. Jameel, A Smart Tower Crane to Mitigate Turbulent Wind Loads, Struct. Eng. Int. 8664 (2019). https://doi.org/10.1080/10168664.2019.1668334.

[59] T.G. Mara, Effects of a construction tower crane on the wind loading of a high-rise building, J. Struct. Eng. 136 (2010) 1453–1460. https://doi.org/10.1061/(ASCE)ST.1943-541X.0000243.

[60] D. Voisin, G. Grillaud, C. Solliec, A. Beley-Sayettat, J.L. Berlaud, A. Miton, Wind tunnel test method to study out-of-service tower crane behaviour in storm winds, J. Wind Eng. Ind. Aerodyn. 92 (2004) 687–697. https://doi.org/10.1016/j.jweia.2004.03.005.

[61] H. Jiang, Y. Li, Dynamic Reliability Analysis of Tower Crane with Wind Loading, IOP Conf. Ser. Mater. Sci. Eng. 677 (2019). https://doi.org/10.1088/1757-899X/677/5/052031.

[62] A.W.T. Leung, C.M. Tam, Prediction of hoisting time for tower cranes for public housing construction in Hong Kong, Constr. Manag. Econ. 17 (1997) 305–314.

https://doi.org/10.1080/014461999371510.

[63]   C.M. Tam, A.W.T. Leung, D.K. Liu, Nonlinear models for predicting hoisting times of tower cranes, J. Comput. Civ. Eng. 16 (2002) 76–81. https://doi.org/10.1061/(ASCE)0887-3801(2002)16:1(76).

[64]   P. Zhang, F.C. Harris, P.O. Olomolaiye, Computer-based model for optimizing the location of a single tower crane, Build. Res. Inf. 24 (1996) 113–123. https://doi.org/10.1080/09613219608727511.

[65]   P. Zhang, P.O. F. Harris, G. Holt, Location Optimization For A Group Of Tower Cranes, 1 (1999) 115–122.

[66]   C.M. Tam, C. Tong, Genetic Algorithm For Optimizing Supply Locations Around Tower Crane, 127 (2001) 315–321.

[67]   C.M. Tam, T.K.L. Tong, GA-ANN model for optimizing the locations of tower crane and supply points for high-rise public housing construction, Constr. Manag. Econ. 21 (2003) 257–266. https://doi.org/10.1080/0144619032000049665.

[68]   K. Alkriz, J.-C. Mangin, A new model for optimizing the location of cranes and construction facilities using genetic algorithms, Assoc. Res. Constr. Manag. ARCOM 2005 - Proc. 21st Annu. Conf. 2 (2005) 981–991.

[69]   C. Huang, C.K. Wong, C.M. Tam, Optimization of tower crane and material supply locations in a high-rise building site by mixed-integer linear programming, Autom. Constr. 20 (2011) 571–580. https://doi.org/10.1016/j.autcon.2010.11.023.

[70]   M.A. Abdelmegid, K.M. Shawki, H. Abdel-Khalek, GA optimization model for solving

tower crane location problem in construction site s, Alexandria Eng. J. 54 (2015) 519–526. https://doi.org/10.1016/j.aej.2015.05.011.

[71]   C. Huang, R. Li, Y. Fu, J. Guo, An Optimizing Algorithm for Tower Crane Selection in Precast Concretes Structures Based on Cost in China, 163 (2018) 1444–1448. https://doi.org/10.2991/iceesd-18.2018.262.

[72]   A. Tubaileh, Working time optimal planning of construction site served by a single tower crane, J. Mech. Sci. Technol. 30 (2016) 2793–2804. https://doi.org/10.1007/s12206-016-0346-8.

[73]   M. Hosseini, P. Beiranvand, M.R. Dadgar, A. Olfati, A mathematical model for optimal tower crane layout planning, Decis. Sci. Lett. 6 (2017) 377–386. https://doi.org/10.5267/j.dsl.2017.2.001.

[74]   A. Kaveh, Y. Vazirinia, Tower cranes and supply points locating problem using CBO, ECBO, and VPS, Int. J. Optim. Civ. Eng. 7 (2017) 393–411. http://ijoce.iust.ac.ir/article-1-305-en.html.

[75]   A.E. Husin, D. Priyanto, Lean Construction Based Tower Crane Requirement Optimization In High Rise Building Construction Project, 7 (2018) 738–743.

[76]   S. Monghasemi, M.R. Nikoo, J. Adamowski, Sequential ordering of crane service requests considering the pending times of the requests: An approach based on game theory and optimization techniques, Autom. Constr. 70 (2016) 62–76. https://doi.org/10.1016/j.autcon.2016.06.006.

[77]   D. Briskorn, M. Dienstknecht, Covering polygons with discs: The problem of crane

selection and location on construction sites, Omega. (2019) 102114.
https://doi.org/10.1016/j.omega.2019.102114.

[78] A. Younes, M. Marzouk, Tower cranes layout planning using agent-based simulation
      considering activity conflicts, Autom. Constr. 93 (2018) 348–360.
      https://doi.org/10.1016/j.autcon.2018.05.030.

[79] D. Lee, H. Lim, H. Cho, K.-I. Kang, Optimization of Luffing-Tower Crane Location in
      Tall Building Construction, J. Constr. Eng. Proj. Manag. 5 (2015) 7–11.
      https://doi.org/10.6106/jcepm.2015.5.4.007.

[80] J. Irizarry, E.P. Karan, Optimizing location of tower cranes on construction sites through
      GIS and BIM integration, Electron. J. Inf. Technol. Constr. 17 (2012) 361–366.

[81] M. Marzouk, A. Abubakr, Decision support for tower crane selection with building
      information models and genetic algorithms, Autom. Constr. 61 (2016) 1–15.
      https://doi.org/10.1016/j.autcon.2015.09.008.

[82] Z.S. Moussavi Nadoushani, A.W.A. Hammad, A. Akbarnezhad, Location Optimization of
      Tower Crane and Allocation of Material Supply Points in a Construction Site Considering
      Operating and Rental Costs, J. Constr. Eng. Manag. 143 (2017) 1–13.
      https://doi.org/10.1061/(ASCE)CO.1943-7862.0001215.

[83] Y. Ji, F. Leite, Optimized Planning Approach for Multiple Tower Cranes and Material
      Supply Points Using Mixed-Integer Programming, 146 (2020).
      https://doi.org/10.1061/(ASCE)CO.1943-7862.0001781.

[84] L.C. Lien, M.Y. Cheng, Particle bee algorithm for tower crane layout with material

117

quantity supply and demand optimization, Autom. Constr. 45 (2014) 25–32. https://doi.org/10.1016/j.autcon.2014.05.002.

[85]   C. Trevino, M. Abdel-Raheem, Single Tower Crane Allocation Using Ant Colony Optimization, Civ. Eng. 3 (2017) 326–334. https://doi.org/doi:10.1061/9780784407943.

[86]   F. Sadeghpour, M. Andayesh, The constructs of site layout modeling: An overview, Can. J. Civ. Eng. 42 (2015) 199–212. https://doi.org/10.1139/cjce-2014-0303.

[87]   S. Hasan, Decision Support System for Crane Selection and Location Optimization on Construction Sites, University of Alberta, 2013.

[88]   S.A. Dudani, The Distance-Weighted k-Nearest-Neighbor Rule, (n.d.) 325–327.

[89]   A. Singh, A. Yadav, A. Rana, K-means with Three different Distance Metrics, Int. J. Comput. Appl. 67 (2013) 13–17. https://doi.org/10.5120/11430-6785.

[90]   W. Chen, X. Qin, Z. Yang, Effects of installation location on the in-service wind load of a tower crane, Proc. Inst. Civ. Eng. - Struct. Build. 173 (2018) 1–16. https://doi.org/10.1680/jstbu.18.00015.

[91]   R. Gallagher, A.C. Elmore, Monte Carlo simulations of wind speed data, Wind Eng. 33 (2009) 661–673. https://doi.org/10.1260/0309-524X.33.6.661.

[92]   S. Hasan, H. Zaman, S. Han, M. Al-Hussein, Y. Su, Integrated Building Information Model to Identify Possible Crane Instability caused by Strong Winds, (2013) 1–10. https://ascelibrary.org/doi/pdf/10.1061/9780784412329.129.

[93]   H.I. Shapiro, J.P. Shapiro, L.K. Shapiro, Cranes and Derricks, 2000.

[94]   A.S. Mikhail, Height extrapolation of wind data., 107 (1982) 10–14.

[95]   A.G. Davenport, Gust loading factors, J. Struct. Div. 93 (1967) 11–34.